Continental Shelf Research 275 (2024) 105198

Contents lists available at ScienceDirect

Continental Shelf Research

journal homepage: www.elsevier.com/locate/csr

Model of Pleistocene geomorphological evolution in active Alpine neotectonics controlled margins in the western Mediterranean area: The case of SE Iberian Peninsula

Trinidad Torres [a], José E. Ortiz [a,*], Rosa Mediavilla [b], Juan I. Santisteban [c], Ana Blázquez [d], Francisco J. Sierro [e], Yolanda Sánchez-Palencia [a], Ignacio López Cilla [a], Rogelio de la Vega [a]

[a] Laboratorio de Estratigrafía Biomolecular, E.T.S.I. Minas y Energía de Madrid, Universidad Politécnica de Madrid, C/ Ríos Rosas 21, 28003, Madrid, Spain
[b] Instituto Geológico y Minero de España (IGME, CSIC), C/Ríos Rosas 23, 28003, Madrid, Spain
[c] Facultad de Ciencias Geológicas, Universidad Complutense de Madrid, C/ José Antonio Novais 12, Ciudad Universitaria, 28040, Madrid, Spain
[d] Institute of Environment and Marine Science Research (IMEDMAR), Universidad Católica de Valencia, C/ Guillem de Castro, 94, 46003, Valencia, Spain
[e] Dept. de Geología, Univ. de Salamanca, Plaza de los Caídos s/n, 37008, Salamanca, Spain

ARTICLE INFO

Keywords:
Pleistocene
Borehole
Marine geophysics
Paleoenvironmental analysis
AAR
Raised marine deposits

ABSTRACT

At the northern tip of the Betic realm (SE Iberian Peninsula), some troughs (synclines) and elevations (anticlines) alternate, marking the present-day coastal lobed morphology of cape-bounded bays, where subsidence and uplift conditions prevailed, respectively. In this study, we were able to establish a clear coastal evolution. To this end, we considered the sedimentological and palaeoenvironmental conditions, the palaeogeographical reconstruction, and recent tectonics until Middle Pleistocene times (MIS 5) through the interpretation of onshore cores, raised marine deposits and geophysical profiles. In this regard, as reflected by both onshore and offshore information, there seems to be a stratigraphical gap from the end of the Pliocene to MIS 15 (Middle Pleistocene). In areas under uplift conditions, linked to tardive Alpine tectonics, the deposits of ancient shorelines and raised beaches were located at different post-depositional elevations, which were dated from odd MIS 15 to MIS 5 using amino acid racemization. Only deposits aged MIS 7 and MIS 5 are roughly at the present-day sea level or some meters above. In the troughs, which remain mostly as lagoons and salt marshes, subsidence did not allow the sedimentary record to be discerned. However, many borehole cores were recovered, attesting lagoonal, marsh, sabkha, or alluvial environmental conditions, which were usually unconnected from the sea. Micropaleontological and amino acid racemization dating revealed these cores to be of MIS15 to MIS5 age. Offshore seismic research revealed five erosive-bounded deposits that are stacked accretionary prisms corresponding to highstands between odd MIS 15 and MIS 5. In contrast, even MISs can be correlated to the erosive horizons that separated the seismic units, reflecting lowstands. In this regard, some bars, at a range of distances from the present-day coastline, protected wetlands from marine influence, allowing the development of diverse subenvironments under changing paleogeographical and paleoclimatological conditions.

1. Introduction

Knowledge of the processes in coastal areas and their evolution is key to the prospective of climate change, variations in sea level, and geological risks, among other factors. The coastal evolution of the Mediterranean realm of the Iberian Peninsula during the Pleistocene and Pliocene has been widely studied. Pleistocene coastal wetlands and marshes in this area provide the only remaining evidence of the satellite basins that developed after the Alpine Orogeny. These coastal environments are associated with marine-terrestrial transition settings, and thus they hold both environmental signals and can be used to link marine and terrestrial records. In this regard, these coastal deposits are commonly linked to changes in sea level in such a way that lowstands are reflected in stratigraphical gaps. However, the record can be considered continuous during periods of active sedimentation.

The Mediterranean coast of Spain has been widely used for the paleoenvironmental reconstruction of Quaternary times. Such studies focused mainly on raised marine deposits linked to highstands during

* Corresponding author.
E-mail address: joseeugenio.ortiz@upm.es (J.E. Ortiz).

https://doi.org/10.1016/j.csr.2024.105198
Received 6 March 2023; Received in revised form 1 February 2024; Accepted 5 March 2024
Available online 12 March 2024

interglacial periods (Goy et al., 1986; Hearty, 1986, 1987; Hearty et al., 1986; Hillaire-Marcel et al., 1986; Causse et al., 1993; Fumanal et al., 1993; Viñals, 1995a, 1995b; Zazo, 1999; Torres et al., 2000, 2010; Ortiz et al., 2004a; Zazo et al., 2003). The main drawback of these studies was age calculation in an area subjected to highly and locally variable recent tectonics (Alfaro Garcia et al., 1995; 1999, 2002, 2012). U/Th dating on mollusk shells (Dumas, 1981; Hillaire-Marcel et al., 1986; Causse et al., 1993) and the presence of paleontological markers (*Persististrombus latus* Gmelin) of Eemian stage (Dumas, 1981; Baena et al., 1982; Goy et al., 1986; Goy and Zazo, 1988) appeared to partially solve this issue. However, radioactive dating on mollusk shells is considered unreliable because these shells are geochemically open systems (Kaufman et al., 1971; McLaren and Rowe, 1996). In addition, markers formerly considered stratigraphical were reclassified as climato-stratigraphical as they were detected in coastal deposits of different ages, at least in MIS 5 and MIS 7 (Goy et al., 1986; Hearty et al., 1986; Hillaire-Marcel et al., 1986; Causse et al., 1993; Zazo, 1999; Zazo et al., 2003; Torres et al., 2006; 2010). The wide use of the amino acid racemization (AAR) dating method allowed identification at the MIS level but could not easily discriminate MIS sub-stages (Hearty et al., 1986; Hearty, 1987; Torres et al., 2013).

Given the flat topography of the coastal area, it is not possible to obtain samples from outcrops, with the exception of raised marine deposits, which are discontinuous. Therefore, it is necessary to use data from boreholes, which in most cases are drilled for other purposes, namely for geotechnical and hydrogeological research, and offshore seismic profiles.

The following basins have been examined in the Spanish Mediterranean realm: Peñíscola (Usera et al., 2006); Torreblanca (Collado and Robles Cuenca, 1983; Segura et al., 1997); Jávea (Fumanal et al., 1993; Usera et al., 2002); Gandía and La Safor (Viñals, 1995a); Moraira (Viñals 1995b); and Albufereta (Blázquez and Ferrer 2003; Ferrer et al., 2005). However, they all have short sequences that cover only the Holocene.

Long coastal records are scarce, and only in the Elche Basin (Fig. 1) have numerous boreholes been drilled and studied in detail (Blázquez, 2005; Blázquez and Usera, 2010), following previous drilling campaigns focusing on the Holocene evolution (Soria et al., 1999). These cores are up to 30 m long but present several gaps and thus do not provide a continuous record. Their microfossil content, together with sedimentological and magnetic susceptibility, allowed the reconstruction of the paleoenvironmental evolution during the Quaternary of the Elche lagoon area (SE Spain). Stratigraphical records from boreholes drilled for hydrogeological studies performed by the Spanish Geological Survey (IGME-CSIC, 2022) are available, together with data from some studies (Santisteban et al., 2004; Blázquez, 2005; Santisteban and Mediavilla, 2006; Mediavilla López et al., 2007; Tabares et al., 2009; Duque et al., 2018).

Offshore seismic research is costly. Offshore morphology (Perea et al., 2012) reveals accretion prisms linked to highstands, as well as paleo-shorelines after lowstands. Fortunately, to conduct the present study, we had access to high-resolution single-channel seismic sparker system profiles (Catafrau et al., 1994; Perea et al., 2012), as well as a commercial seismic profile (Archivo Técnico de Hidrocarburos).

Thus, using data from "mainland deposits", edge of sea deposits, and offshore deposits, here we sought to: (1) establish the complete Pleistocene chronological framework of the area between Roig Cape and Huertas Cape (Alicante) through AAR of long cores and new raised marine deposits; (2) determine the paleoenvironmental conditions of

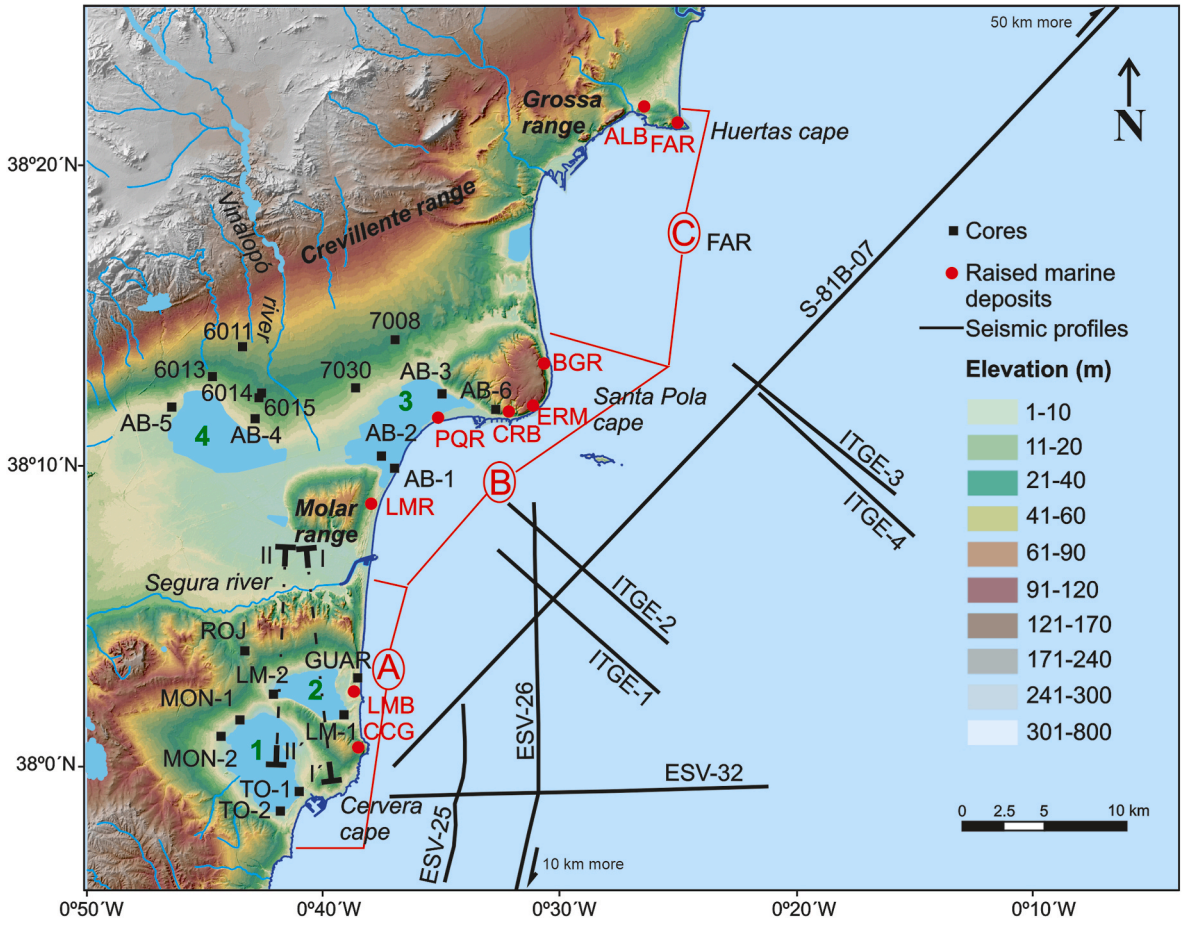

Fig. 1. Digital Terrain Map (DTM) of the study area. Offshore seismic profiles, raised marine deposits and onshore cores are indicated. 1: Torrevieja lagoon; 2: La Mata lagoon; 3: Pinet salt works; 4: El Hondó marsh.

the area and the location of the coastline during highstands; and (3) reinterpret some seismic profiles and expand on the information derived from them to link all the morphologies for the first paleogeographical reconstruction.

2. Geographical and geological settings

The study area is in the province of Alicante (Eastern Spain) (Fig. 1). Four capes or headlands, namely Huertas, Santa Pola, Cervera, and Roig, all of them tectonic-related, mark off the existence of lowlands where the lagoonal and alluvial deposits predominate at present. We differentiated three dominions on the basis of their morphostructural characteristics (Fig. 1).

A Roig Cape-Segura river mouth.

The most striking characteristics are the Torrevieja (14 km^2) and La Mata lagoons (7 km^2) in the vicinity of Cervera Cape. South of this headland, the coastline consists of a continuous cliff attesting to a tardive neotectonics-linked uplift, while to the north a wide sandy beach extends tens of kilometers until the Segura river mouth.

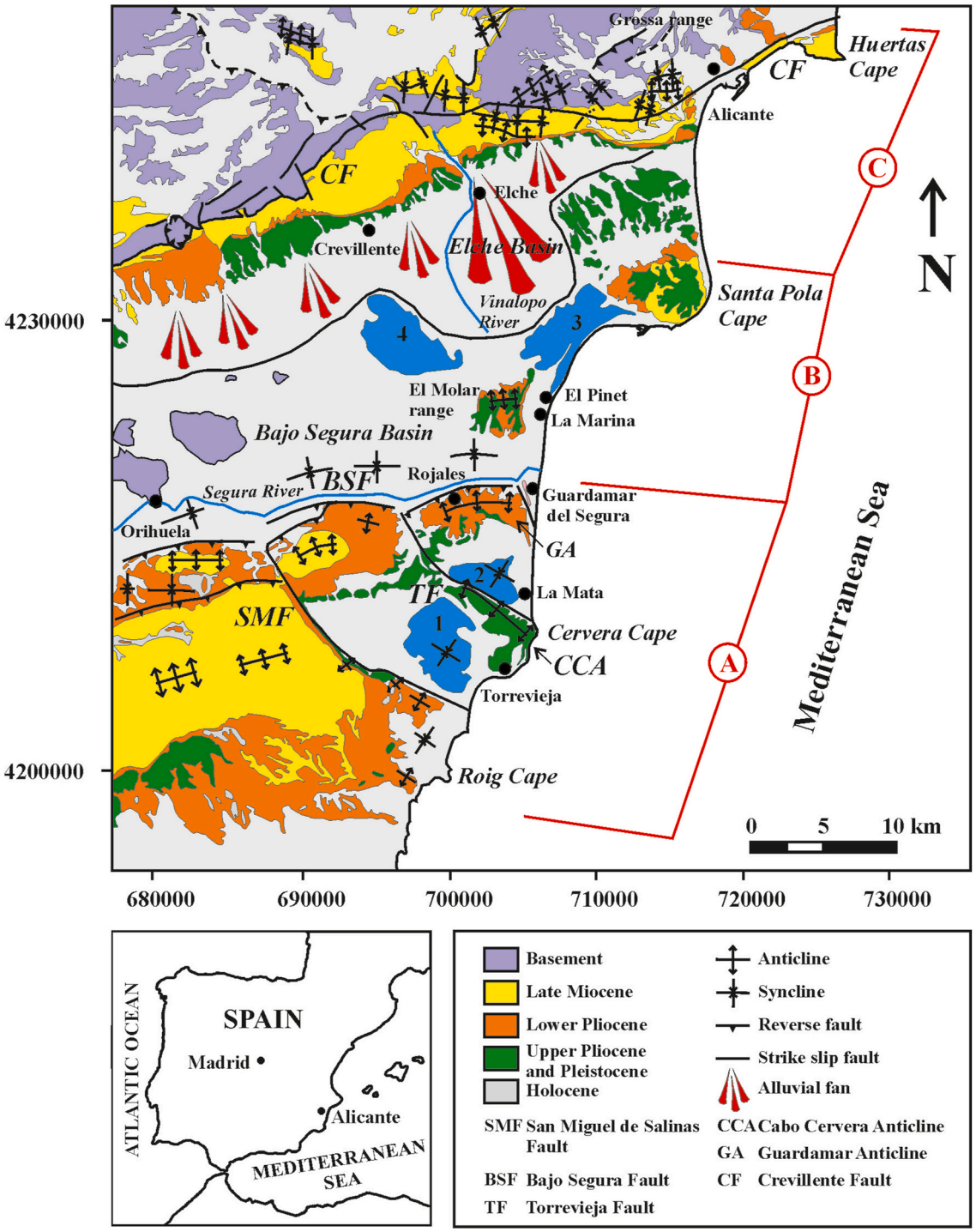

Fig. 2. Geological map of the study area. 1: Torrevieja lagoon; 2: La Mata lagoon; 3: Pinet salt works; 4: El Hondó marsh.

B Segura river mouth-Santa Pola Cape.

Northwards of the Rojales Highs, until Santa Pola Cape, the Segura river appears, together with its associated alluvial plain and delta. The area located to the north evolves into gently sloped bajadas built by alluvial fans with their apices at the Crevillente range, the Vinalopó river being the most important watercourse. These alluvial deposits correspond to the final Holocene infill stage of the *Sinus Ilicitanus* (Elche Basin). Two strongly anthropized marshes characterize the area: el Hondó, located inland, and the Pinet salt works, on the coast. A small elevation (Molar range) can be described as the natural division between the fluvial and alluvial fan dominion.

C Santa Pola Cape-Huertas Cape (Alicante Bay)

This area extends from the Santa Pola Cape to Las Huertas Cape, which is characterized by a wide and protected bay delimited to the north by the Crevillente and Grossa ranges. Both terrestrial and marine environments are strongly anthropized, making it very difficult to determine the pristine geography of the area. At the s northern tip of the study area is Las Huertas Cape.

2.1. Geology

The study area is located in the Bajo Segura and Elche zones in the Eastern Betic realm (Fig. 2), between the African and Iberian plates (Fontán et al., 2013), in the so-called Eastern Betic Shear Zone (Alfaro et al., 2015). During the Alpine Orogeny, the basin underwent NNW-SSE horizontal compression (Montenat et al., 1990; Martín-Martín et al., 2020), which created a wide syncline to the south (sectors A and B in Fig. 2), the Crevillente anticline, and the Alicante Trough at the northern tip of the study area (sector C in Fig. 2). Minor structures (anticlines) located at Cervera Cape, Rojales, El Molar range, and Santa Pola Cape compartmentalize the synclines.

Giménez et al. (2009) and García-Mayordomo et al. (2012) defined strike-slip faults of regional development in the area (Fig. 2), namely the San Miguel de Salinas (SMF), Torrevieja (TF), Bajo Segura (BSF), and Crevillente (CF) Faults, which condition the present-day landscape (Silva et al., 1993). These faults show a notable continuity in the offshore dominion (Perea et al., 2012) and, according to the Quaternary Faults Database of Iberia (QAFI, García-Mayordomo et al., 2012), they are still active—a property reflected by the marked seismicity of the zone during historical times (Martinez Solares and Mezcua Rodriguez, 2002). According to Somoza (1993), and based on raised beach markers, seismicity in the area caused vertical movements between 0.2 and −0.2 mm year. Seismic-lined deformation structures are frequent in the area (Alfaro et al., 1999). In fact, Torres et al. (2022) proposed that the TF, the BSF or a set of faults linked to the former, affecting the Upper Pleistocene aeolian sediments of Cervera Cape were probably linked to the historical Torrevieja earthquake.

The Elche Basin has been widely studied (Fumanal et al., 1998; Ferrer and Blázquez, 1999; Blázquez et al., 2000; Blázquez, 2005; Blázquez and Usera, 2010; Dabrio et al., 2011; Tent-Manclús, 2013). It consists of a wide and flat area between the Segura River to the south and the Crevillente range to the north; the small elevation of the Molar range (La Marina) acts as a divide between the Lower Vinalopó Basin and the wider Elche Basin.

Regrettably, there is a lack of stratigraphy, and the age of the Quaternary infill is only known from geophysical research that focused on older and deeper formations. Along the Uppermost Pleistocene and Holocene, the Elche Basin appeared to be, at least in its easternmost part, connected to the Mediterranean Sea and was named *Sinus Ilicitanus* during Roman times. Relics of these conditions are the brackish-water marshes of Clot de Galvany and El Fondó, and probably the Pinet salt works near the sea. Active alluvial fan activity was responsible for the massive silting of the aquatic realm (Blázquez, 2005; Alfaro et al., 2015; Silva et al., 2015; Segura-Beltrán and Pardo-Pascual, 2019; Tent-Manclús, 2012; Tent-Manclús et al., 2014; Tent-Manclús and Soria, 2014). The Holocene record has a thickness of ca. 10 m (Alfaro et al., 1999; Soria et al., 1999; Cuenca et al., 2000), showing frequent processes of liquefaction and convolute bedding, attesting to high seismicity.

Many raised beach deposits have been described and dated along this coastline (Zazo et al., 2003; Dabrio et al., 2011; Torres et al., 2013, 2022). The oldest ones belong to Lower-Middle Pleistocene and, after successive neotectonics-raising processes, are usually preserved on the sea-face headland (anticlines), while on the flat areas, subsidence processes sunk these deposits to different depths. Raised beach deposits linked to odd MISs are observable along the present-day coastline (La Mata, La Marina, Santa Pola Cape, and Huertas Cape) (Torres et al., 2013, 2020, 2022). However, many of them have been destroyed as a result of the "tourist resort fever" over the last 50 years.

The present-day lowlands reflect the Pleistocene infill of pre-existing depressed areas with subsequent evolution to lagoonal environments, and little is known about their age, thickness, or facies, although data derived from paleoseismic characterization (Alfaro et al., 2012) are available. Knowledge of the offshore Pleistocene record obtained through seismic profiles lacks detail since these studies focused on older materials (Palaeogene or Mesozoic) for commercial purposes (Archivo Técnico de Hidrocarburos), or information is limited (Catafrau et al., 1994).

3. Materials and methods

Here we used samples from long records. However, Pleistocene onshore deposits, with the sole exception of the Rojales section (ROJ), were not directly observable, making it necessary to study, when available, cores drilled in the area. In Sector A, a considerable number of boreholes were drilled by the Spanish Geological Survey (TO-1, TO-2, MON-1, MON-2, LM-1, LM-2, and GUAR; Fig. 1), and the cores were kept at the Peñarroya storage facility. They were sampled according to the different observed lithologies. However, we did not directly study the borehole records from Sectors B and C as, in most cases, the cores were not recovered, although we had access to lithologs (6011, 6013, 6014, 6015, 7008, 7030) (IGME-CSIC, 2022) and published results (Blázquez, 2005). In this regard, in 1996, six boreholes with continuous core recovery (AB-1 to AB-6) were drilled in the Elche Basin. These were carefully described and interpreted by Blázquez (2005), although numerical datings were carried out on materials that lacked reliability. Here we included new age data from one of these boreholes (AB-2).

Due to the different chrono-stratigraphical attributions, we also performed a stratigraphical section in the municipality of Rojales, named ROJ, which was previously studied by Goy et al. (1990), Montenat et al. (1990), and Soria et al. (1996). Its age was a matter of debate, and here we solve this question.

In the cores from Sector A and AB-2, we selected samples for AAR analysis. To establish the age of the Rojales Sandstone Formation (Fm) and also the correlation of the stratigraphical records, we also used some samples from cores MON-1, GUAR, and TO-2, and the ROJ section for both $^{87}Sr/^{86}Sr$ isotope and biostratigraphical dating.

To obtain a chronological framework of the geological processes that determined the geomorphological evolution of the area, we also performed AAR dating on selected *Glycymeris* shells from three raised marine deposits: La Marina-2 (LMR-2), Carabineros (CRB) and Ermita (ERM). In the locality named Pinet quarry (PQR), we were unable to find *Glycymeris* sp. shells for AAR dating purposes, and *Arca noae* individuals were therefore used instead and their their D/L ratios were converted to *Glycymeris*-equivalent ones, following Hearty et al. (1986).

We also considered the ages of other raised marine deposits that outcrop in the area, which were reported by Torres et al. (2000) in ALB-1, ALB-2, FAR-A, FAR-C, and FAR-D, by Ortiz et al. (2004a) and Torres et al. (2013) in LMR-1, by Torres et al. (2013) in BRG, and by Torres et al. (2022) in CCG and LMB.

To obtain a general framework of the Quaternary sedimentary processes that occurred in this area, high resolution offshore seismic profiles were also considered (Fig. 1), namely ITGE-1, ITGE-2, ITGE-3 and ITGE-4 (Catafrau et al., 1994), and EVS-32, EVS-26, EVS-25 (Perea et al., 2012), as well as the commercial seismic profile S-81B-07 (Archivo Técnico de Hidrocarburos). Here we expand on the discussion by Perea et al. (2012) and focus mainly on paleo shoreline positions along different lowstands, as well as the identification of unconformity linked to highstand-related deposits. In addition, we reinterpreted the seismic profiles reported by Catafrau et al. (1994).

3.1. Sedimentology and paleontology

To examine the sedimentological and palaeontological content, samples of ca. 50 g were dried at room temperature for 48 h and water-dispersed. They were passed through a 150-μm sieve and then dried and weighed. Examination under a microscope allowed the determination of the sedimentological and microfossil (ostracode, foraminifera, and micro-mollusk) content.

Macro- (mollusks) and micro-fossils (foraminifera, ostracodes) were identified at the genus level and sometimes at the species level. For mollusk identification, we used the atlases of D'Angelo and Gargiullo (1987) and Gofas et al. (2011). To identify ostracode species, we used the studies of Carbonel (1985) and Guillaume et al. (1985). Planktonic foraminifera were identified following Kennet (1983), Loeblich and Tappan (1988), Hemleben et al. (2012), Hayward et al. (2017), and Schiebel and Hemleben (2017). In addition, the biostratigraphical framework of Lirer et al. (2019) was followed to determine the Pliocene ages.

3.2. Strontium isotope dating

Five levels belonging to the Rojales Sandstone Fm. consisting of yellow sands were analyzed: two from the low part of the ROJ stratigraphical section containing foraminifera tests and mollusks (*Ostrea* and *Pecten*), a sample made of mollusks from the MON-1 core (MON-1-178.2), and samples containing benthic foraminifera tests from the GUAR (GUAR-84.4) and the bottom of core TO-2 (TO-2-139.5).

The samples were picked and then cleaned by sonication in distilled de-ionized (DDI) water. The $^{87}Sr/^{86}Sr$ isotope ratios were measured using a fully automated Thermal Ionization Mass Spectrometer (TIMS, Phoenix). Strontium was separated from the samples by ion exchange chromatography. The laboratory work was carried out by the analytical facilities at James Hutton Institute, Aberdeen. Two SRM 987 international standards and one in-house Holocene Marine Carbonate standard (HMC) were analyzed alongside the samples to monitor the QC of the complete analytical procedure (HMC) and mass spectrometer performance (SRM987 and HMC). The standard results are consistent with published values and the long-term average values for the laboratory. The Sr Stratigraphy Age Dates were determined from the measured $^{87}Sr/^{86}Sr$ isotope ratios by reference to Howarth and McArthur (1997) Look-Up Table Version 4: 08/04 (latest version June 2006). The minimum and maximum age dates were based on the ±2SE of the measured $^{87}Sr/^{86}Sr$ isotope ratios and the confidence limits of the calibration curve. The timescale of Gradstein et al. (2004) was used.

3.3. Amino acid racemization dating

Selected samples from the cores were washed and sieved at 63 μm, and ostracode carapaces and mollusk shells were recovered under a binocular microscope. We used a total of 156 ostracode valves (analytical samples) from 36 beds of cores from Sector A and core AB-2, and 2 gastropod shells from 2 beds of cores MON-1 and MON-2. The ostracode valves were carefully cleaned by sonication in DDI water and rinsed to remove sediment. They were then submerged for 3 h in hydrogen peroxide to eliminate organic matter. Of note, the use of monogeneric samples reduces taxonomically controlled variability in D/L values (Murray-Wallace and Goede, 1995; Murray-Wallace and Goede, 1995). Only clean and translucent valves of the species *Cyprideis torosa* (Jones) were selected from each bed, with the exception one sample containing valves belonging to *Herpetocypris reptans* Baird. In addition, 29 *Glycymeris* shells from LMR-2, CRB, and ERM localities, and 6 *Arca noae* Linneo shells from PQR were sampled for AAR dating.

To avoid recent contamination (recent algae and/or decay products of other organisms), mollusk shells were picked from the sea whenever possible. A hollow diamond drill was used to remove a discoid sample (8 mm in diameter) from an area close to the beak. A small sample was taken near the aperture of gastropod shells belonging to the Helicidae family in samples from cores MON-1 and MON-2. In all cases, peripheral parts (approximately 20–30%) were removed after chemical etching with 2 N HCl. Afterwards, 10–20 mg of samples was used for AAR analysis.

Later, ostracode valves were hydrolyzed under an N_2 atmosphere in 7 mL of 6 M HCl for 20 h at 100 C, whereas 20 mL/mg of 7 M HCl was used for mollusks. The hydrolysates were evaporated to dryness in vacuo and then rehydrated in 7 mL (ostracodes) or 10 mg/mL (mollusks) 0.01 HCl with 1.5 mM sodium azide and 0.03 mM L-homo-arginine (internal standard).

Amino acid concentrations were quantified using high-performance liquid chromatography, following the sample preparation protocol described in Kaufman and Manley (1998) and Kaufman (2000). Samples were injected into an Agilent HPLC-1100 liquid chromatograph equipped with a fluorescence detector. Excitation and emission wavelengths were programmed at 230 nm and 445 nm, respectively. A Hypersil BDS C18 reverse-phase column (5 μm; 250 × 4 mm i.d.) was used for the analysis. HPLC analysis was performed following the LEB routine (Ortiz et al., 2013), which allowed the separation of D/L forms of aspartic acid (Asx), glutamic acid (Glx), serine (Ser), glycine (Gly), alanine (Ala), valine (Val), phenylalanine (Phe), isoleucine (Ile), leucine (Leu), threonine (Thr), arginine (Arg), and tyrosine (Tyr).

Numerical ages were obtained for ostracode and land snails since age calculation algorithms were developed by Ortiz et al. (2004) and Torres et al. (1997), respectively. For marine mollusks (*Glycymeris* and *Arca noae*) dating was performed at the MIS level by comparison of D/L values with those of Aminozones established for the Mediterranean realm (Hearty et al., 1986; Hearty, 1987; Torres et al., 2013).

4. Results

4.1. Chronology

The numerical ages obtained by the $^{87}Sr/^{86}Sr$ isotope ratio are shown in Table 1. Of note, all the samples were dated at the Pliocene or Miocene, as expected. Indeed, the presence of planktonic foraminifer tests of species of clear stratigraphical value confirmed these ages (Table 2).

With these results, we addressed the age of the ROJ section (which some authors considered as belonging to the Pliocene) representing the Pliocene transgression after the Messinian crisis of evaporite sedimentation (Caracuel et al., 2011).

According to Goy and Zazo (1989), the lowest 15 m, which consists of yellow sands (Rojales Sandstone Fm.), are of Pliocene age, while the rest of the section (Variegated Sandstones and Marls Fm., and Segura Conglomerates Fm.) belongs to the Pleistocene. Bardají et al. (1995) attribute the yellow sands of the Rojales Sandstone Fm. to the Pleistocene, whereas the gray-blue marls (Hurchillos marl Fm.) that appear below them, belong to the Pliocene. In contrast, based on Montenat et al. (1990) and Soria et al. (1996), the whole ROJ section is of Pliocene age (except the uppermost conglomerates, which belong to the Pleistocene according to Montenat et al., 1990). Our results showed that the age of the Rojales Sandstone Fm. ranged from 2.36 to 5.96 Ma (Table 1), confirming the ages proposed by Soria et al. (1996) through the study of

Table 1
$^{87}Sr/^{86}Sr$ isotope ratios in some levels of cores TO-2, GUAR and MON-1, and Rojales (ROJ) section with their corresponding ages.

Level	Depth (m)	Taxa	$^{87}Sr/^{86}Sr$	±2SE	Age (Ma)	Max. Age (Ma)	Min. Age (Ma)
TO-2-139.5	139.5	forams	0.709058	0.000006	3.40	4.39	2.65
GUAR-84.4	84.4	forams	0.709024	0.000007	5.38	5.62	5.08
MON-1-178.2	178.2	mollusc frag.	0.709046	0.000005	4.60	4.91	3.92
ROJ-78.0	78.0	mollusc frag.	0.708996	0.000004	5.96	6.06	5.85
ROJ-78.0	78.0	forams	0.709074	0.000024	2.36	4.53	1.57

Table 2
Biostratigraphical dating of some levels of cores MON-1 and TO-2 belonging to the Rojales Sandstone Fm.

Level	Foraminifera association	Age
MON-1-172.0	*Ammonia*, *Nonion*, *Textularia*, *Globigerina bulloides*, *Neogloboquadrina* sin., *Gblobigerina apertura*, *Globigerinoides extremus*	>3.17 Ma probably older than 4.2 My
MON-1-178.2	*Ammonia*, *Nonion*, *Elphidium*, *Melonis*, *Globigerina bulloides*, *Globigerina apertura*, *Globigerinoides extremus*	>3.17 Ma probably older than 4.2 My
MON-1-184.4	*Ammonia*, *Nonion*, *Elphidium*, *Lobatula*, *Globigerina bulloides*, *Globigerina apertura*, *Globorotalia sciltula* dex., *Neogloboquadrina pachyderma sin. & dex. Globigerinoides inmaturus*	4.2–8.3 Ma probably Lower Pliocene (5.3–4.2 My)
TO-2-139.5	*mmonia*, *Nonion*, *Elphidium*, *Lobatula*, *Gyroidina*, *Uvigerina*, *Neogloboquadrina pachyderma* dex., *Globigerina bulloides*, *Globigerinoides ruber*, *Globigerina apertura*, *Globigerinoides inmaturus*, *Globorotalia scitula* sin., *Globorotalia margaritae*	5.2–3.85 Ma. Lower Pliocene

microvertebrate remains.

The mean D/L values of Asx and Glx in ostracode valves from the beds of the cores and their corresponding ages are shown in Table 3. To establish the numerical ages of samples used for AAR, we selected these amino acids because they account for a significant percentage (>50%) of the total amino acid content of most ostracode valves (Kaufman, 2000; Bright and Kaufman, 2011; Ortiz et al., 2013). The numerical ages of the beds were determined by introducing the Asx and Glx D/L values obtained in ostracode valves collected at each level into the age calculation algorithms established by Ortiz et al. (2004b). In general, the numerical datings obtained were consistent with depth.

For Helicidae, we also selected Asx and Glx D/L values as they also account for a significant percentage of the amino acid content for most gastropods (Goodfriend, 1991; Torres et al., 1997). In gastropod samples (Helicidae), the D/L values of Asx and Glx were introduced into the age calculation algorithms of Torres et al. (1997) for central and southern Iberian Peninsula.

The age of a single bed is the average of the numerical dates obtained for each amino acid D/L value measured in gastropods or ostracodes from that level, and the age uncertainty is the standard deviation of the numerical ages calculated at each level.

The mean D/L values of three amino acids (Ile, Asx and Glx) in *Glycymeris* shells of LMR-2, CRB and ERM, and *Arca noae* shells from PQR are given in Table 4. These amino acids are the most reliable ones in these taxa (Torres et al., 2000, 2013). In samples from PQR, the D-aIle/L-Ile ratio was obtained from *Arca noae* individuals and converted into *Glycymeris* D-aIle/L-Ile values using a *Glycymeris/Arca* ratio of 1.31 (Hearty et al., 1986). Thus, the samples from Pinet quarry showed similar racemization and epimerization values to those from raised marine terraces of MIS 5e age (Aminozone E of Hearty et al., 1986; Hearty, 1987). Similar D/L values were also reported by Torres et al. (2000, 2010, 2013), Ortiz et al. (2017) and De Santis et al. (2018, 2020) for MIS 5 deposits in the Mediterranean realm. In contrast, samples from CRB and ERM showed similar D/L values and correlated with MIS 7 (Aminozone F of Hearty et al., 1986; Hearty, 1987), whereas

Table 3
Aspartic acid (Asx) and glutamic acid (Glx) D/L values in ostracode valves of levels from some cores with their corresponding ages.

Level	Taxa	N	D/L Asp	D/L Glu	Age (ka)	MIS
GUAR-6.0	*C. torosa*	1	0.619	0.386	507.4 ± 56.3	13
LM-1-23.3	*C. torosa*	4	0.605 ± 0.080	0.293 ± 0.061	433.6 ± 170.7	11
LM-1-24.0	*C. torosa*	6	0.626 ± 0.067	0.315 ± 0.084	478.2 ± 186.4	11
LM-2-29.6	*C. torosa*	1	0.650	0.483	627.2 ± 15.6	15
LM-2-34.8	*C. torosa*	5	0.664 ± 0.035	0.551 ± 0.051	768.8 ± 124.3	15
LM-2-35.7	*C. torosa*	5	0.669 ± 0.040	0.449 ± 0.074	638.5 ± 134.9	15
LM-2-35.9	*C. torosa*	5	0.676 ± 0.013	0.502 ± 0.014	689.0 ± 54.9	15
LM-2-38.0	*C. torosa*	6	0.651 ± 0.041	0.504 ± 0.055	653.1 ± 102.5	15
LM-2-39.5	*C. torosa*	6	0.632 ± 0.021	0.490 ± 0.062	609.1 ± 84.5	15
LM-2-40.2	*C. torosa*	6	0.658 ± 0.025	0.503 ± 0.081	662.2 ± 98.3	15
LM-2-40.6	*C. torosa*	6	0.636 ± 0.025	0.556 ± 0.084	674.3 ± 142.4	15
TO-2-11.9	*C. torosa*	2	0.490	0.181	233.2 ± 63.6	7
TO-2-12.3	*C. torosa*	5	0.460 ± 0.137	0.245 ± 0.045	302.0 ± 69.1	7
MON-2-66.8	Helicidae	1	0.821	–	442.8	11
MON-2-89.8	*H. reptans*	3	0.641	0.434	575.7 ± 52.1	13
MON-2-95.3	*C. torosa*	3	0.634 ± 0.024	0.437 ± 0.100	572.1 ± 111.6	13
MON-1-10.9	*C. torosa*	5	0.622	0.314	461.7 ± 136.0	13
MON-1-29.5	*C. torosa*	5	0.580 ± 0.059	0.328 ± 0.018	421.3 ± 90.7	13
MON-1-36.8	*C. torosa*	5	0.563 ± 0.099	0.411 ± 0.130	477.3 ± 187.3	13
MON-1-50.0	*C. torosa*	5	0.613 ± 0.100	0.341 ± 0.133	493.3 ± 241.5	13
MON-1-52.3	*C. torosa*	4	0.579 ± 0.057	0.372 ± 0.102	455.0 ± 124.1	13
MON-1-53.4	*C. torosa*	3	0.546	0.420	447.6 ± 99.1	13
MON-1-58.9	*C. torosa*	5	0.561 ± 0.028	0.337 ± 0.057	404.4 ± 63.2	13
AB-2-0.9	*C. torosa*	6	0.497 ± 0.031	0.257 ± 0.044	293.0 ± 47.1	9
AB-2-7.1	*C. torosa*	6	0.486 ± 0.048	0.268 ± 0.068	331.2 ± 92.0	11
AB-2-7.2	*C. torosa*	2	0.569 ± 0.027	0.375 ± 0.011	439.3 ± 37.9	11
AB-2-8.0	*C. torosa*	6	0.531 ± 0.047	0.254 ± 0.057	409.4 ± 3.9	11
AB-2-14.0	*C. torosa*	6	0.613 ± 0.046	0.453 ± 0.092	562.0 ± 110.4	13
AB-2-14.5	*C. torosa*	6	0.535 ± 0.016	0.395 ± 0.093	470.2 ± 127.3	13
AB-2-16.7	*C. torosa*	5	0.579 ± 0.078	0.329 ± 0.047	424.9 ± 119.6	13

Table 4
Mean D/L values of isoleucine, aspartic acid, glutamic acid obtained in *Glycymeris* shells of the different localities. D-aIle/L-Ile values, which were analyzed in HPLC, are presented as equivalent GC values. In PQR D-aIle/L-Ile ratios were obtained in *Arca noae* speciments and they were converted into *Glycymeris* D-aIle/L-Ile values (put into brackets) using a *Glycymeris/Arca* ratio of 1.31 (Hearty et al., 1986).

Site	Taxa	N	D-aIle/L-Ile	D/L Glu	D/L Asx	Age
LMR-2	*Glycymeris*	9	0.930 ± 0.058	0.782 ± 0.042	0.860 ± 0.030	MIS 11
CRB	*Glycymeris*	10	0.605 ± 0.058	0.427 ± 0.068	0.519 ± 0.099	MIS 7
ERM	*Glycymeris*	10	0.595 ± 0.071	0.567 ± 0.042	0.668 ± 0.073	MIS 7
PQR	*Arca*	6	0.368 ± 0.047 [0.482 ± 0.061]	0.400 ± 0.036	0.618 ± 0.041	MIS 5

LMR-2 belonged to MIS 11.

4.2. Sedimentology

Based on the descriptions of the stratigraphical records (cores and ROJ section) and the lithological and paleontological descriptions of samples studied under the microscope, we identified several facies, which were differentiated on the basis of grain size, color, sedimentary structures, and mineral and fossil content. These units were based on Santisteban and Mediavilla (2006) and are shown in Fig. 3 and in more detail in Table 1 in the Supplementary information.

CS-Coastal sabkha/palustrine: characterized by the presence of gypsiferous (lenticles) black muds and contained *Chara* oogonia, root marks, botryoidal pyrite, charcoal, and hydromorphic marks.

CM-Coastal marsh: consisted of brown/white carbonate mud with scattered gypsum lenticles and contained a paucispeciphic fossil association of *C. torosa* and *Ammonia beccarii* (Linneo) and *Chara* oogonia.

AM-Alluvial: formed by red muds with variable amounts of sand, and incipient caliche formations. Occasionally brown, azoic sands were dominant.

CA-Caliche: characterized by tiny laminated massive or nodular, calcium carbonate accumulations and did not contain fossil remains and was affected by microkarsts.

BE-Beach and bar (Upper Shoreface): consisted of heterometric quartz and carbonate sands with frequent presence of bioclasts of thick-shelled mollusks, pelecypoda, and gastropoda.

LG-Lagoon: made of fine-very fine quartz sand, with centimeter-thick coquina beds, benthic foraminifera, and *C. torosa.*

MLG-Marine lagoon: characterized by cream-colored carbonate mud with low quartz sand content and presence of well-preserved mollusk shells: *Cerastoderma*, *Mitylaster*, *Hydrobia*, together with *Chara* (various species) oogonia, ostracods (mainly *C. torosa*), and benthic foraminifera (*Ammonia, Lobatula*).

EO-Eolian: consisted of very fine quartz and carbonate sand grains, containing highly eolized flaky tiny-shelled clasts and benthic foraminifera tests.

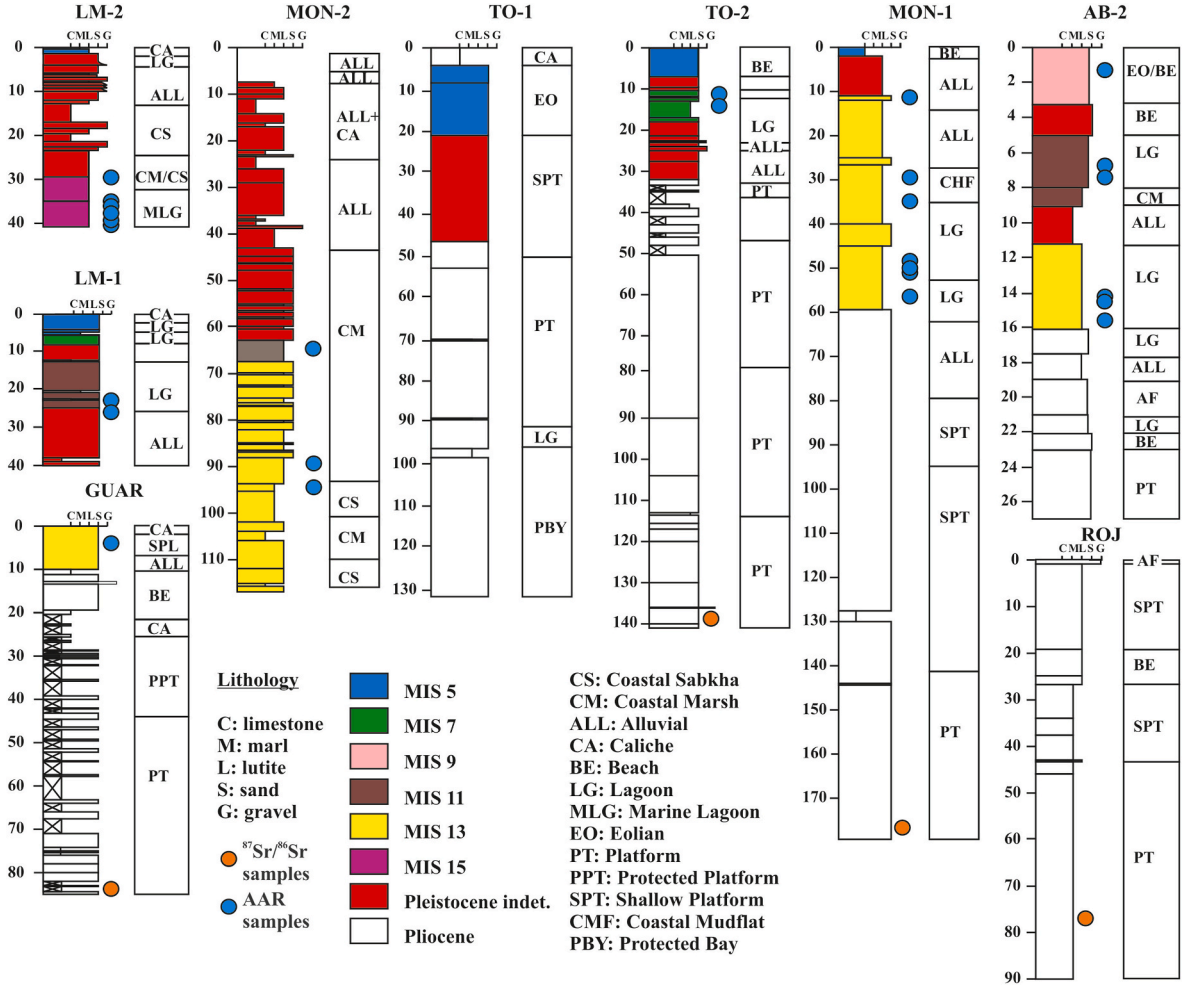

Fig. 3. Facies interpretation and AAR ages from LM-1, LM-2, GUAR, MON-1, TO-1 and TO-2 cores and Rojales stratigraphic section (ROJ). A short interpretation of AB-2 core record was included (modified from Blázquez 2005). The position of the samples dated by $^{87}Sr/^{86}Sr$ (Table 1) and AAR (Table 3) is included.

PT-Marine platform (only for Pliocene age sediments): made of greenish very fine sand, with ripples, high bioturbation, and scarce mollusk remains.

PPT-Marine protected platform (only Pliocene age sediments): characterized by medium/coarse-grained cross-bedded sands, carbonate cemented, with charcoal, phytoclasts, bioclasts, and molds from mollusk.

SPT-Shallow platform (only Pliocene sediments): consisted of yellow silty mud, with ripples, pyrite, and abundant mollusk remains.

CMF-Coastal mudflat (only in Pliocene records): made of marborized-brown mud without fossil remains.

PBY-Protected bay (only Pliocene sediments): characterized by fine sand, silt, and clay, showing cross-bedding, ripples, and parallel lamination, with the presence of planktonic and benthic foraminifera tests, pelecypoda shells, and fish bones and teeth.

5. Discussion

5.1. Long continuous records

The numerical ages obtained by the $^{87}Sr/^{86}Sr$ isotope ratios and the micropaleontological study of planktonic foraminifera revealed and confirmed that the ROJ section and the bottom of the core records from Sector A had a clear Pliocene age, forming the "basement" of the Pleistocene infills of La Mata and Torrevieja Basins (Fig. 3). These sediments accommodated in a synclinal delimited by the Rojales and Torrevieja anticlines. The progressive change to a more terrestrial character towards the top of the sequences was evident, although the full continental Rojales conglomerates were lacking due to erosion or facies alteration. However, we were able to define the structure of Pliocene deposits (Fig. 4), the development of the Torrevieja anticline (core TO-1) and La Mata syncline (cores TO-2, MON-1) being clearly visible, while core GUAR was placed on the southern limb of the Rojales anticline.

Sector B lacks Quaternary material outcropping, except a few raised beach deposits, so the only available data come from boreholes drilled for hydrogeological research (6011, 6013, 6014, 6015, 7008, 7030), the Holocene sedimentation rate through a drilling campaign (Soria et al., 1999), and data from a study performed by Blázquez (2005).

Reaching a depth of ca. 500 m, the IGME boreholes are deeper than those of Soria et al. (1999) and Blázquez (2005). The drilling logs reveal a predominance of gravel, sand, and mud (Table 5), allowing their interpretation to be of alluvial fan origin, probably corresponding with the still active alluvial fans with their apices in the Crevillente range. We estimate that the maximum thickness of these materials was 230 m (IGME-CSIC, 2022), suggesting that this record extends to Pleistocene times. The lack of any kind of dating precludes greater precision. Soria et al. (1999) focused only on Holocene records in which alluvial facies predominated, although brackish water ingressions were determined and were more frequent near the present-day coastline.

Blázquez (2005) studied six cores named AB-1 to AB-6. In almost all the cases, the Quaternary record never surpasses 20 m of total thickness and in two cases (AB-1 and AB-2) these sediments lie unconformably on Pliocene materials (Blázquez, 2005). Of note, cores AB-1 and AB-2 were in clear relation with the Grossa range made of faulted Pliocene deposits.

In these cores, fine-grained sediments deposited in lagoon to marsh environments, predominate, alternating with coarser deposits of alluvial origin (Table 5). Marine deposits were recorded only in core AB-2. Indeed, the ages obtained here (Table 3, Fig. 3) allowed us to interpret that lagoonal conditions prevailed during MIS 9, MIS 11 and MIS 13. In contrast, inland, towards el Hondo marsh, only alluvial sedimentation took place (AB-4 and AB-5; Blázquez, 2005). These observations matched the borehole information (6011, 6013, 6014, 6015, 7008, 7030) of IGME-CSIC (2022).

There is no available underground information from the core record of Sector C. However, based on the geological map (Fig. 2), the deposit of pre-Quaternary age extended almost to the shoreline, leaving little space for the development of Pleistocene inland basins.

A significant number of samples provided clear datings in all cores, thereby allowing correlation between them (Fig. 5) and the establishment of the chronological location of sedimentological facies, thus facilitating further paleographical discussion. In this regard Pliocene deposits in these cores were identified according to the lithological, sedimentary and palaeontological characteristics defined by Santisteban and Mediavilla (2006).

MIS 15 deposits appeared only in core LM-2, which was drilled near La Mata syncline axis. The facies of the units progressively changed upwards from a lagoon with marine influence to a sabkha.

MIS 13 deposits were present in some cores, namely MON-1, MON-2, GUAR, and AB-2. These deposits represented a marine environment (platform) in core GUAR. In contrast, they can be interpreted as lagoon/sabkha/mud flat deposits in MON-1, MON-2 and AB-2. These deposits were affected by recent tectonics. Of note, La Mata fault affects cores MON-1 and MON-2 in such a way that Pliocene deposits were not drilled in the latter, and MIS 13 palustrine deposits appeared much deeper in this core.

MIS 11 deposits appeared in the axial area of La Mata syncline and near the present La Mata Complex Bar (LMB) (core LM-1), as well as in core AB-2. These deposits showed a lagoonal character.

MIS 9 deposits were present only in core AB-2, being of lagoonal character.

MIS 7 deposits were dated in core TO-2, and they presented faunal association, thereby indicating a coastal lagoon. Tiny deposits of this age have been found in the short core named LML (Torres et al., 2022, Fig. 1), which has a clear shallow marine character, as well in core LM-1, representing lagoon deposits.

MIS 5 deposits appeared in core LM-2, attesting to a strong marine

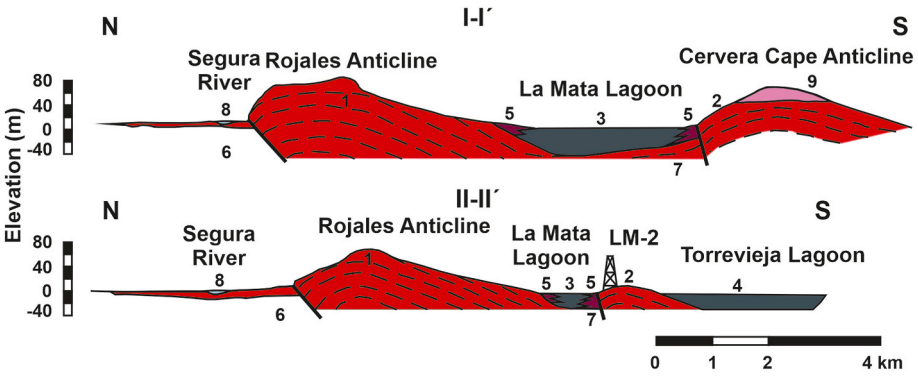

Fig. 4. Schematic deduced La Mata-Torrevieja syncline geometry from Rojales section and core samples that resulted of Pliocene age. 1: Rojales anticline (Pliocene), 2: Torreveja anticline (Pliocene); 3: La Mata lagoon; 4: Torrevieja lagoon; 5: alluvial deposits; 6: Bajo Segura Fault; 7: La Mata Fault; 8: Segura river; 9: eolian deposits.

Table 5
Short description of the core records drilled in Bajo Segura-Elche Basin (after Blázquez, 2005; IGME-CSIC, 2022).

Core	Elevation a.s.l. (m)	Depth (m)	Lithology	Environment
6014 (IGME-1)	40	90	Mud, gravel with muddy matrix	Alluvial
6013 (IGME-2)	20	151	Gravel, mud	Alluvial
6011 (IGME-3)	42	10	Gravel, sand, mud	Alluvial
7008 (IGME-4)	33	19.25	Mud and gravel	Alluvial
7030 (IGME-5)	38	57	Clay, silt, gravel	Alluvial
6015 (IGME-6)	40	500	Sandy mud (0–230 m)	Alluvial
			Blue & gray marl & silt (230–500 m)	Marine Pliocene
AB-1 (Salinas)	1	30	Sands (0–5.5 m)	Marine Beach (MIS 1)
			Sands (5.5–10.0 m)	Marine (MIS 1/MIS 5)
			Mud and sand (10.0–17.0 m)	Alluvial/palustrine
			Sand and silt (17.0–30.0 m)	Marine Pliocene
AB-2 (Pinet)	1	36	Sands (0–3.0 m)	Beach/eolian (MIS9)
			Muddy sands (3.0–5.0 m)	Marine
			Sandy muds (5.0–8.0 m)	Lagoon (MIS 11)
			Muds (8.0–9.0 m)	Palustrine (MIS 11)
			Muds (9.0–11.2 m)	Alluvial
			Limestones & muds (11.2–16.0 m)	Lagoon (MIS 13)
			Mud, gravel, sand (16.0–18.0 m)	Backbarrier
			Limestones (18.0–19.0 m)	Palustrine
			Mud, sand (19.0–21.0 m)	Washover fan
			Sand (21.0–22.0 m)	Beach/eolian
			Gravel, sand (22.0–23.0 m)	Mesolitoral Pliocene
			Sand (23.0–30.0 m)	Marine Pliocene
AB-3 (Mórtoles)	2	31	Mud & sands (0–8.5 m)	Alluvial/lagoon (MIS 1)
			Sands (8.5–9.5 m)	Beach (MIS 5)
			Sands & mud (9.5–19.2 m)	Alluvial (MIS 9)
			Sands (19.2–19.8 m)	Marine
			Sands & mud (19.8–32.0 m)	Alluvial
AB-4 (Fondó)	8	12	Gray muds (0–3.5 m)	Palustrine (MIS 1)
			Red sand muds (3.5–7.2 m)	Alluvial (MIS 1)
			Gray muds (7.2–12.0 m)	Palustrine (MIS 1)
AB-5 (Riegos)	9	8	Gravel, mud and sand	Alluvial (MIS 1)
AB-6 (Picola)	2	23	Sands (0–2.8 m)	Marine (MIS 1)
			Silty sands (2.8–5.5 m)	Backbarrier (MIS 1)
			Sands & reef limestone	Pliocene

influence with abundant mollusk remains. Of note, core LM-2 was drilled 4.5 km westward of LML where MIS 5 age deposits cropped along the “El Acequión” ditch walls.

5.2. Raised marine deposits

The raised marine deposits of the Pleistocene of Sector A were represented mainly by La Mata Complex Bar (LMB) and some thick and extensive coquina-like deposits, which were extensively described by Somoza et al. (1986) and Zazo et al. (1990), and dated by Torres et al. (2022) at MIS 5 and MIS 7 (Fig. 6). These deposits corresponded to the sandy bar that protected La Mata and Torrevieja lagoons from direct sea influence. In this area, it is also worth noting the deposits in the area of Cervera Cape, which contained large amounts of *Glycymeris* shells (CCG) accumulated by a tsunami that occurred at MIS 5 (Torres et al., 2022).

In Sector B, close to La Marina village, Torres et al. (2013) described two raised marine deposits named LMR-1 and LMR-2 (Fig. 6). These should not be confused with those of Goy et al. (2003), named PQR here. LMR-2 consisted of carbonate-cemented bioclastic sands with scarce well-preserved fossils, thereby pointing to an upper shoreface environment. LMR-1 deposits consisted of silt, and fine-grained sands with large amounts of *Cladocora coespitosa* (Linneo) individuals in life position overlaid by gravel with abundant *Glycymeris* sp. shells, representing a deeper marine environment. U/Th dating on coral samples and AAR dating on *Glycymeris* shells indicate that they belong to MIS 11 (Fig. 6; Ortiz et al., 2004a; Torres et al., 2013).

Next to the Pinet salt works, there is a quarry in which five strongly cemented sandstone beds outcrop (8.5–9.0 m a.s.l.) from an ancient spit bar (PQR) in which gravels were common, together with abundant *P. latus* representatives, *Arca* shells and *C. caespitosa* (Fig. 6). AAR ages obtained here confirmed that PQR belonged to MIS 5 (Bernat et al., 1982; Hillaire-Marcel et al., 1986; Hearty et al., 1986), although Goy et al. (2003) suggested that this locality was of MIS 7.

In Sector C, the area of Santa Pola Cape has been of interest because of the presence of several raised marine terraces (Gaibar-Puertas and Barceló, 1969; Montenat, 1973, 1977; Bellés et al., 1978; Dumas, 1981; Echailler and Lauriat, 1978; Zazo et al., 1981; Goy and Zazo, 1987, 1988; Hearty et al., 1986).

In this area, some raised beach levels were identified and dated here. BGR-3 (+15 m) and BGR-4 (+20 m) contained large numbers of well-preserved *Glycymeris* representatives in a sandy carbonate matrix dated at MIS 13 (Fig. 6; Torres et al., 2013). CRB and ERM were also located in this area and were dated at MIS 7.

At the northern tip of Alicante Bay, two raised marine beach deposits (Albufereta 1-1 and Albufereta 1–2) appeared to belong to MIS 7 and MIS 5, respectively (Fig. 6). Of note, deposits belonging to MIS 5 appeared at a higher elevation than those of MIS 7.

Huertas Cape is, in a wide sense, the northern boundary of the Lower Segura Basin. Three marine deposits were found at different elevations: FAR-A (29 m a.s.l) dated at MIS 11, and FAR-C (1 m a.s.l) and FAR-D (0.4 m a.s.l.) (Fig. 6), both dated at MIS 5 (Torres et al., 2000). Only FAR-C presented a high faunal diversity while only *Glycymeris* shells appeared in the other two raised deposits.

5.3. Offshore deposits

The commercial MCS profile S-81B07 from Exxon (Archivo Técnico de Hidrocarburos) sheds light on the offshore tectonic arrangement of the area, although the main chrono-stratigraphical units are defined as Upper Miocene, Pliocene, and Quaternary (Fig. 7). This seismic profile was partially interpreted by Perea et al. (2012), and here we complete the interpretation. The structures are arranged as a succession of troughs and highs that landwards correspond to more or less complex synclines and anticlines. At the north part of the seismic profile, the deep Alicante

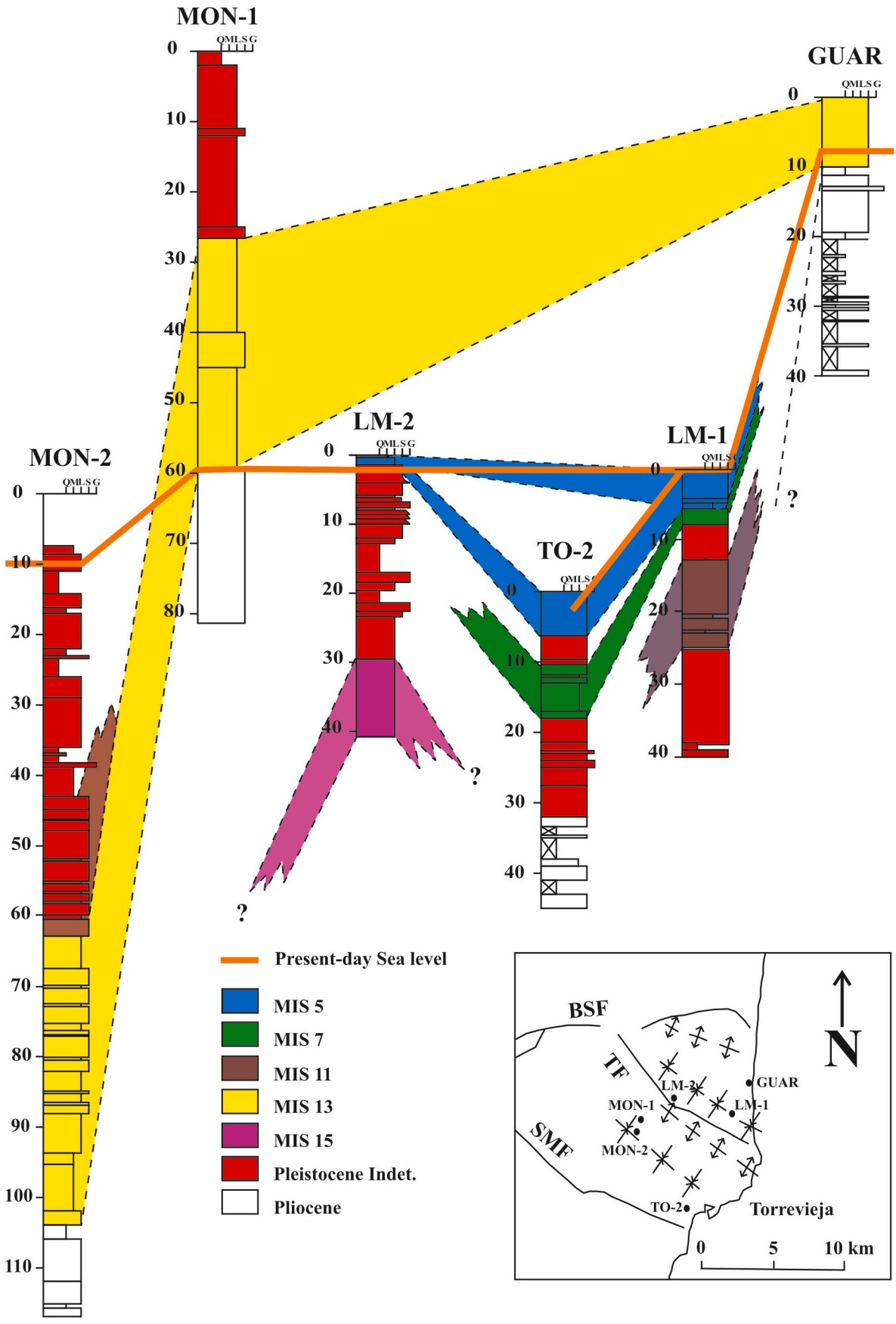

Fig. 5. Correlation of the long records from La Mata zone.

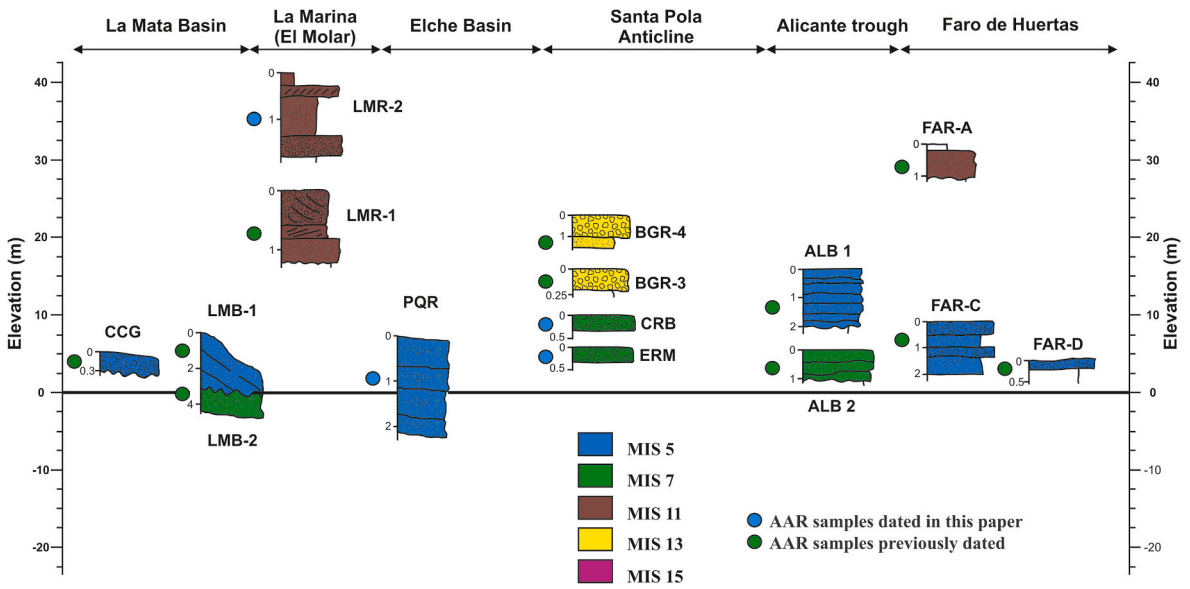

Fig. 6. Age and present-day elevation of raised beach deposits at the edge of the sea in the study area. CCG and LMB (Torres et al., 2022); LMR-1 (Ortiz et al., 2004a; Torres et al., 2013), BRG: Torres et al. (2013); ALB-1, ALB-2, FAR-A, FAR-C and FAR-D: Torres et al. (2000). Ages from LMR-2, PQR, CRB and ERM were obtained here. The position of the samples dated by AAR (Table 4) is included.

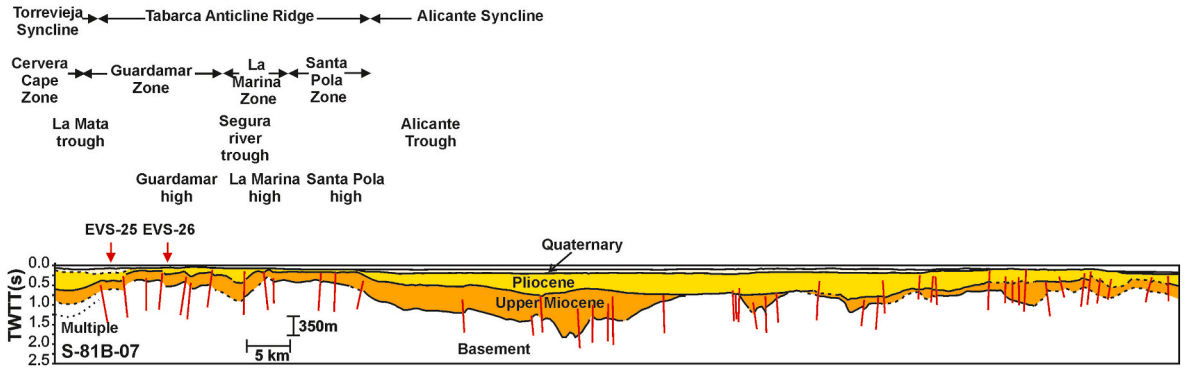

Fig. 7. Interpreted commercial seismic profile S-81B-07 from Exxon with the different dominions and sub-dominions differentiated (partially based on Perea et al., 2012).

Trough stands out, which is finally enclosed by the Huertas Cape high (Fig. 7).

Perea et al. (2012) used the results from an offshore seismic campaign focused on the identification of Quaternary active tectonic structures in the Bajo Segura Basin, as well as the identification of different seismo-stratigraphical units bounded by horizons that correspond to regional erosional surfaces linked to main lowstands. In fact, they described the accretion prism and the position of the paleo-shoreline. As no drilling or coring was scheduled during the offshore geophysics campaign, those authors considered the units described by Rabineau et al. (2006). Thus, based on a seismo-stratigraphical study in the area of La Mata, and following the age model of Rabineau et al. (2006) for the Lyon Gulf (western Mediterranean), Perea et al. (2012) established six units (I1-I6) linked to highstands separated by large erosional surfaces (H1-H5) which occurred during lowstands (Fig. 8, Table 6). No special considerations were made about the identification of the sedimentary units.

This interpretation was supported by the curves of sea-level oscillation proposed by several authors (Imbrie et al., 1984; Labeyrie et al., 1987; Skene et al., 1998; Shackleton, 2000; Lambeck and Chappell, 2001; Waelbroeck et al., 2002 among others), suggesting general seawater flooding during odd MISs, and erosion linked to decreases in sea level in even MISs.

Thus, the position of the paleo-shoreline during even MISs (MIS 12 to MIS 2), in which lowstands occurred, was identified based on the erosive surface-bounded platform deposits from MIS 13 to MIS 1 (Fig. 8).

In this regard, the linkage between the offshore, edge of sea, and underground Pleistocene record was supported by the identification of the seismic marine units that appeared in the EVS-32 sparker profile that began ca. 2 km offshore from Cervera Cape (Perea et al., 2012). The same units can be identified in S-N running profiles of EVS-25 (ca. 6 km offshore) and EVS-26 (ca. 10 km offshore). In EVS-25, it was possible to identify the same units as in the VS32 sparker profiles that run across the Torrevieja syncline, Torrevieja anticline, and La Mata syncline, allowing observation of a progressive unconformity developed during the Pleistocene that affected mainly the damping of units I6 and I5 upwards. The profile marked the paleotopography of the erosive surfaces, which were characterized by “buttes”, which can be interpreted as being linked to erosion of the underlying formation or relic bars or dunes.

Four geophysical profiles were also published by Catafrau et al. (1994) (Figs. 1 and 9), who observed that the capes correlate with strongly folded and faulted rocks of the Betic External realm, which are, in turn, unconformably covered, through an abrasion surface, by marine sediments of Pliocene age, which are also slightly folded. According to those authors, the maximum thickness of the Quaternary record in the platform reaches 160 m, being higher in the talus area and lower in the

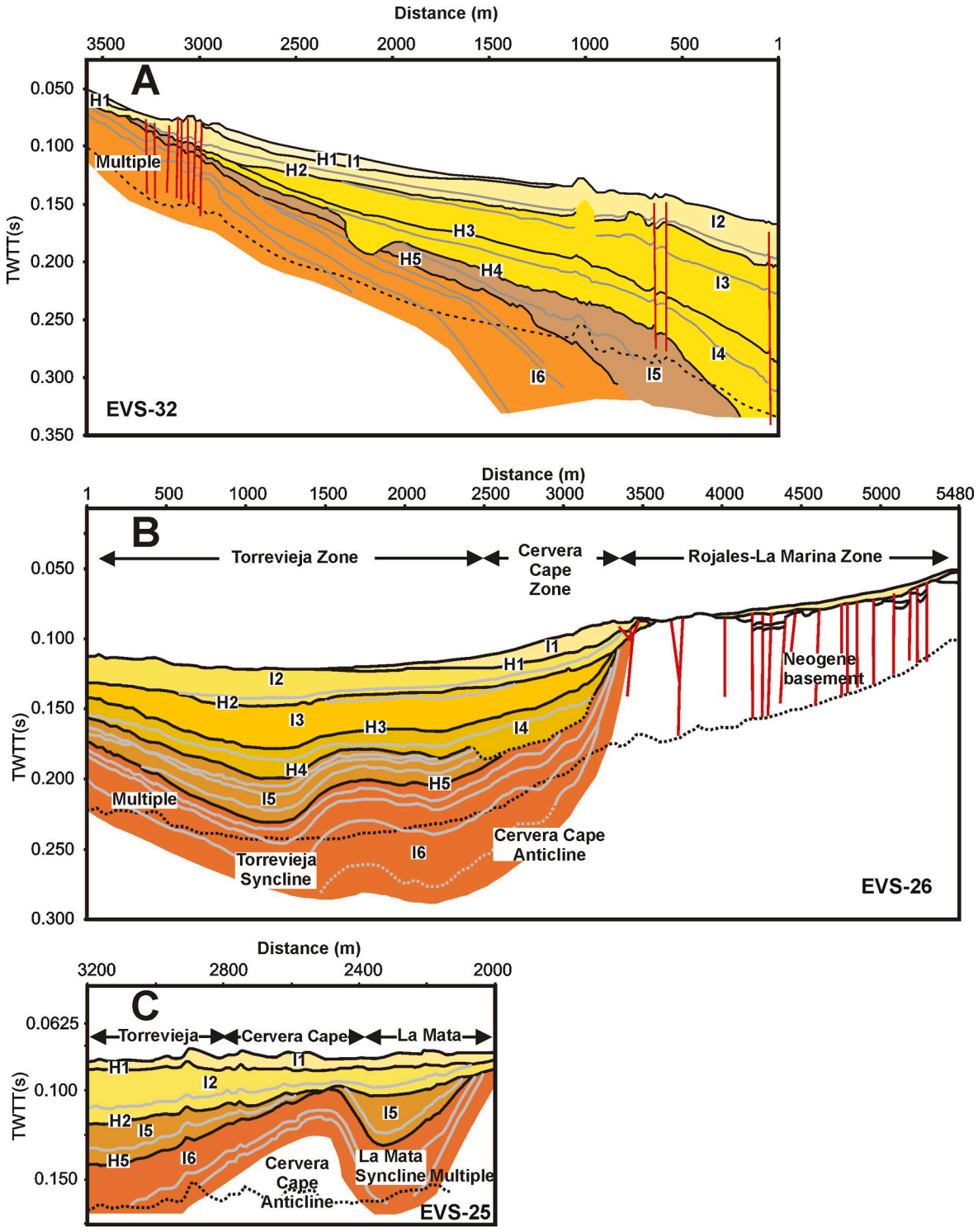

Fig. 8. Interpretation of seismic profiles in La Mata area (modified from Perea et al., 2012): EVS-32, EVS-26 and EVS-25. Seismic units are described in Table 6.

threshold areas, i.e. Santa Pola Cape, where thickness does not surpass 20 m.

Seismic profile ITGE-1 (Fig. 9A) runs in a NW-SE direction (Fig. 1). This section shows thin (<20 m in total thickness) undisturbed Quaternary age marine deposits, which, in turn, fossilize an erosive surface that affects Pliocene age sediments (Catafrau et al., 1994).

Seismic profile ITGE-2 (Fig. 9B) runs parallel to the ITGE-1 profile (Fig. 1). It is possible to observe faulted and folded Pliocene age sediments fossilizing a paleo relief developed on Mesozoic age rocks of the internal Betic realm (Catafrau et al., 1994). Of note, near the NW tip of the profile the thickness of Quaternary age sediments diminishes to 10 m, while in the central part of the profile it thickens markedly. At the SE tip, this profile reveals a butte-like structure, which could reflect an ancient bar. Profile ITGE-2 is aligned with the raised beach deposits of Santa Pola Cape, which have been dated at MIS 13 and MIS 7. However, there are presumably older deposits 80 m a.s.l. that did not provide shell samples for AAR dating.

The seismic profile ITGE-3 (Fig. 9C) reveals a fault-controlled rugged

Table 6
Interpretation and age attribution of the seismic units differentiated by Perea et al. (2012). Erosive boundaries (H) and stratigraphic units (I) identified in EVS-32 profile (based on Perea et al., 2012).

Unit	Description	Inferred Age
I1	It is the thinnest unit. It seems to accommodate into a through parallel to the present day coast bounded landwards by the TF and seawards by a mound that could be made of authigenic carbonate. Eastward from the TF this unit seems to reach the present- day coastline.	MIS 1
H1	Very irregular erosive horizon	MIS 4
I2	This unit apparently reaches the present-day coastline. Two subunits are observable onlapping the oldest units. It shows a clear tinning trend offshore-onshore, but it is markedly affected by the TF swarm many of them reaching the seafloor also producing a net thickening of the unit.	MIS 5
H2	Erosive surface with little topographic contrast. Near the TF an abrupt hummock followed offshore by two small troughs are noticeable	MIS 6
I3	This unit wedges more than 2 km offshore the present day coastline, thickening markedly offshore. It consists on two subunits.	MIS 7
H3	Erosive surface with little topographic contrast. Near the TF there are two small hummocks.	MIS 8.2
I4	This unit wedges more than 2 km the present-day coastline, thickening markedly offshore. It consisted on two subunits	MIS 9
H4	Marked flat erosive surface with a sour at its central part reaching I6 unit deposits.	MIS 10
I5	This unit does not reach the present-day coastline. Wedges near the area affected by the TF. Two subunits are observable.	MIS 11
H5	Slightly erosive surface. Near the Torrevieja anticline, it is affected by faults. Hummock structures developed.	MIS 12
I6	Thicker unit. 4 distinctive subunits.	MIS 13 (+MIS 15)

paleo-relief fossilized by Pliocene age sediments which fill in graben or horst structures and thus show large variations in thickness (Catafrau et al., 1994). The thickness of Quaternary sediments is reduced, ca. 10 m, and in spite of general horizontal arrangement, near the SE tip of the profile they are uplifted. Minor undulations can be interpreted as bars or fossil (?) sand ribbons.

The seismic profile ITGE-4 (Fig. 9D) shows a "normal" platform morphology in which Catafrau et al. (1994) differentiated only three units attributed to the Lower, Middle, and Upper Pleistocene.

Here we interpreted at least six sedimentary units, which can be tentatively correlated to units I1-I6 described by Perea et al. (2012), linked to the platform deposits of MIS 13–15, MIS 11, MIS 9, MIS 7, MIS 5, and MIS 1. Two superimposed bars are visible at the NW tip of the section. Of note, from Fig. 9D, the shoreline during MIS 4 can be interpreted as being linked to the erosive surface located at the top of unit I2.

At least three seismic singularities can be observed (D1-D3), which in some cases conditioned the sedimentation landwards (lagoon ?), being onlapped at its top. D2 shows a local foreshore bedding, while the internal structure of D1 and D3 is not clear. These deposits can be interpreted as bars, encrusted dunes, or bioconstructions. The structure of D2 strongly suggests a bar development while the structures of the other two are unclear.

5.4. General linkage between pleistocene records

The most common evidence of marine deposits in the study area was the upper shoreface detrital sediments made of calcareous/quartz sands, bioclastic sands and gravels with the presence of *Glycymeris* shells and the gastropod *P. latus*. In the area, stacked deposits belonging to MIS 7 and MIS 5 were found in PQR, CRB, ERM, together with LMB-1 and LMB-2 (Torres et al., 2022), and with Albufereta (ALB-1 and ALB-2) (Torres et al., 2000). In contrast, in FAR-C and FAR-D (Huertas Cape), only MIS 5 deposits (Torres et al., 2000) occurred. We propose that these marine raised deposits can be lineally linked (some extrapolation is needed) to their equivalents in the platform dominion.

At the edge of the sea, there was commonly abundant evidence of MIS 5 deposits, such as notched beach deposits (Huertas Cape), barriers (LMB-1, LMB-2), and spit bars (Pinet quarry), which can be correlated to their age-equivalents on the offshore platform.

At La Mata lagoon and closing complex bar, three units were defined from cores and/or outcrops (LMB-1, LMB-2, LML). These were observed and interpreted as overlapping MIS 5 deposits over the previous MIS 7 bar (Torres et al., 2021) in such a way that, in spite of their unidimensional and punctual character, they helped to establish the correlation between marine and lagoonal environments. Indeed, Storms et al.

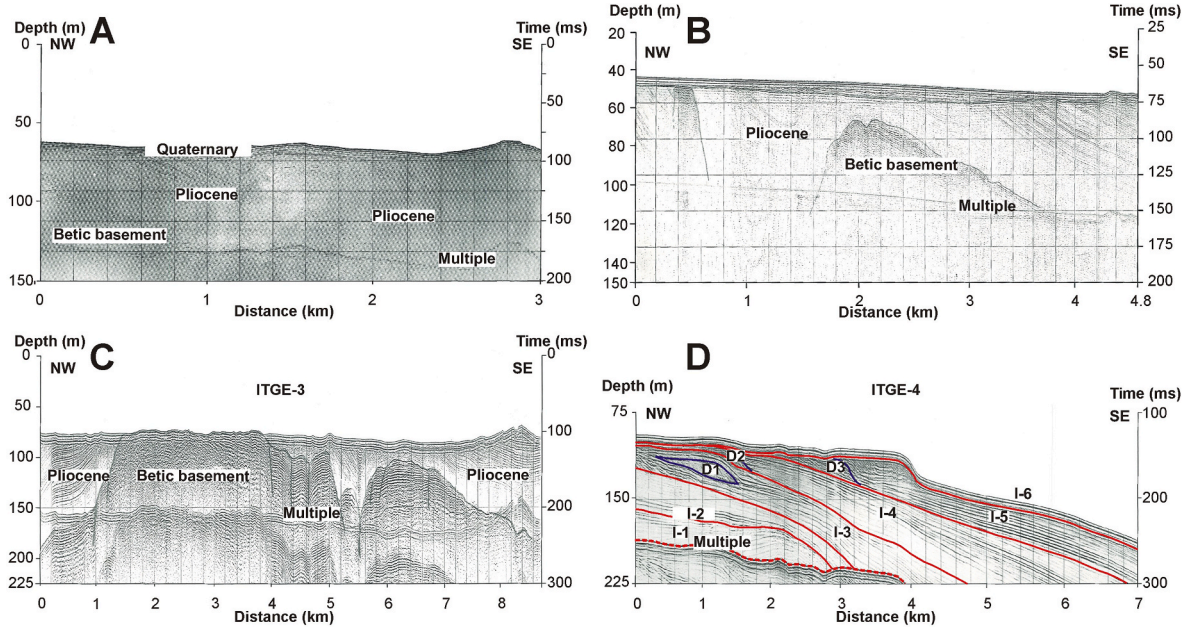

Fig. 9. Offshore seismic profiles covering the Lower-Segura River Basin and Alicante Through zones (after Catafrau et al., 1994): A) ITGE-1, B) ITGE-2, C) ITGE-3, D) ITGE-4. The location of the profiles appear in Fig. 1.

(2008) defined the changes in barrier-lagoon systems in the northern Adriatic shelf, in which older barriers were drowned and destroyed while the younger ones remained reasonably in situ.

In fact, in La Marina realm, Zazo et al. (2003) observed MIS 7 and MIS 5 stacked beach deposits, and Ortiz et al. (2004b) identified ancient MIS 13 low-energy deep water deposits (*Cladocora coespitosa*, a coral, in life position), which are now 35 m above the present sea level.

Marine geophysics in this area indicated that raised beach deposits nested on the sea face of different highs (anticlines) are present in underwater structures (Figs. 8 and 9). Along the present-day coastlines formed by the different troughs (synclines), ancient beach deposits older than MIS 7 are not visible while marine geophysics reveals well-developed platform deposits of the same ages that most certainly consisted of beach units landwards.

However, recent tectonics rejuvenated and faulted previous Alpine folds and consequently markedly uplifted deposits formerly located close to the sea level in the areas of La Marina-Santa Pola Cape and Huertas Cape, where raised beach deposits of MIS 11 and MIS 13 were at ca. 24–40 m a.s.l. (LMR-1 and LMR-2), ca. 20–30 m a.s.l. (BGR-3, BGR-4), and ca. 29 m a.s.l. (FAR-A).

As offshore equivalents of La Marina and Santa Pola are very shallow, there was a visible lack of accommodation space. It is plausible that a general uplift occurred after MIS 11, causing preexisting deposits to be eroded in shallow adjacent marine areas.

The relationships between inland and offshore environments were very clear in some cases, such as in the Elche Basin, Vinalopó sub-basin, and La Mata-Torrevieja lagoons, where the core records revealed an almost complete absence of marine sediments, except for the uppermost part of core LM-2. In all the core records, the fossil-rich muddy beds corresponded to deposits of restricted environments that oscillated between saline-marsh-carbonate marsh/sabkha and coastal plain (Fig. 3) alternating with alluvial deposits. A similar facies distribution was described in core AB-2 (Blázquez, 2005). These observations indicate that these small basins (synclines or troughs) were isolated from the sea from MIS 15 to MIS 5 because of unknown barriers that were built or because the paleo coast during highstands was far enough from these areas. In fact, raised marine deposits belonging to odd MISs (from MIS 13 to MIS 5) occurred throughout this area. The resilience of these sedimentary environments is not rare. In Pego marsh (Valencia), Torres et al. (2014) described a continuous stratigraphical record that extends from MIS 15 to MIS 5, and in the Antas river record, MIS 5 organic-rich muds lie on MIS 11 alluvial deposits (Torres et al., 2015).

The deposits of the top of core LM-2 were a conspicuous exception, and a short marine ingression or an anomalous high-energy event (tsunami) related to the high seismicity of the zone has been postulated by Torres et al. (2022).

Conceptual models of the general paleogeographical trends in the area are shown in Fig. 10 based on considerations derived from general sea level oscillation curves, sedimentological data from the interpretation of the core records, and marine geophysics. It must be highlighted that there is an unavoidable gap between the onshore and the westernmost starting point of the seismic profiles. In addition, it has to be considered that the proposed sea-level curves were used here in a relative manner because of the strong and locally variable intensity of uplift and subsidence rates. Thus, during odd MISs, when sea level rose, wetlands appeared from MIS 15 to MIS 5. According to the sedimentological records of the cores, during the oldest MIS, the extensions of the lagoon, alluvial plain, carbonate marsh, and sabkha facies were not as large as during MIS 7 and MIS 5.

6. Conclusions

At the end of the regressive succession of Pliocene deposits, tardive Alpine tectonics were the origin of the Torrevieja, La Mata, Lower Segura River-Elche Basin synclines, which are interrupted by small anticline structures. The accurate dating of the ROJ section obtained

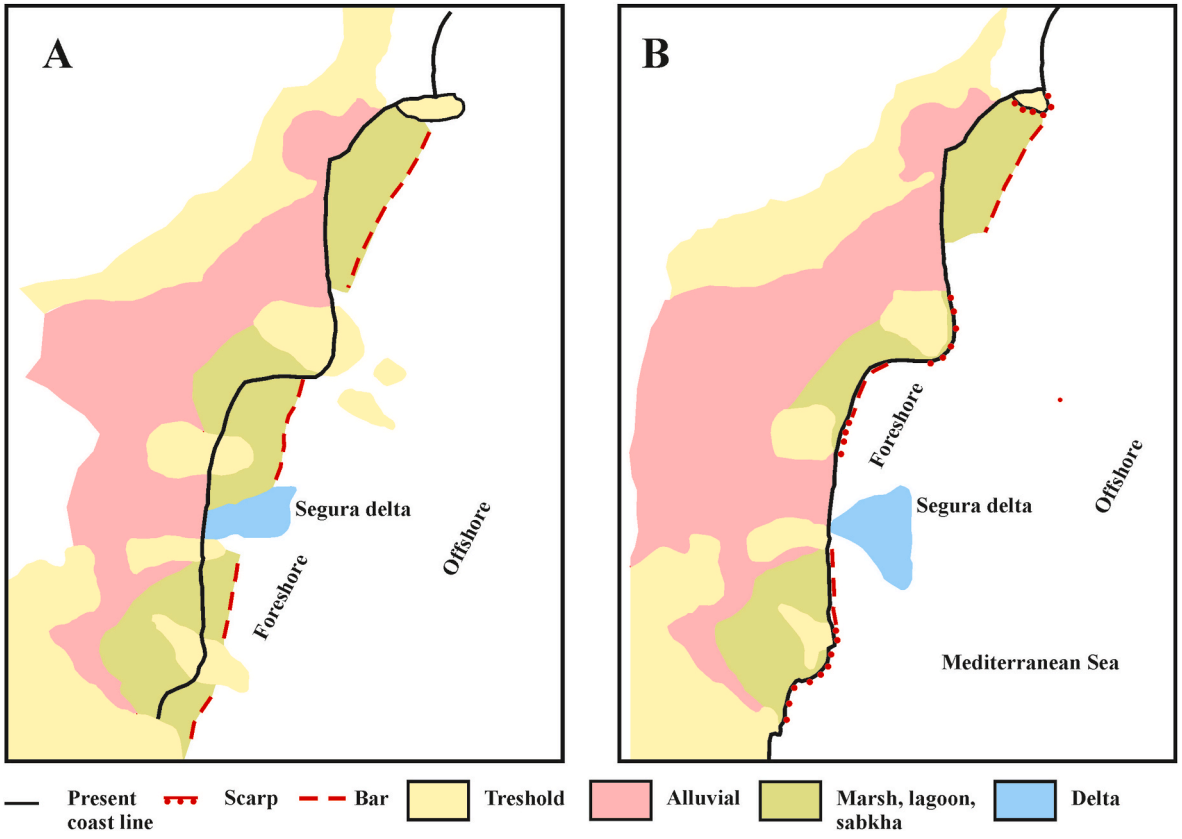

Fig. 10. Palaeogeographical scenarios in area of Alicante with the facies distribution: a) during MIS 9 and MIS 11, and b) during MIS 7 and MIS 5.

here allowed us to determine the true morphology of La Mata Basin. These structures conditioned the coastal morphology during Pleistocene highstands (odd MISs): anticlines projected headland (capes) and synclines hosted wetlands riveted by beaches and bars.

From the marine seismic research, we can interpret that the oldest deposits belonged to MIS 15, in coincidence with onshore data from core samples, such as in LM-2 and Pinet AB-2 cores. This implies that, from the end of Pliocene to MIS 15, erosive conditions and/or non-deposition prevailed onshore, while marine sedimentation took place offshore.

Similarly, seismic units that corresponded to younger odd MISs, which were linked to highstands, can also be correlated with continental records of similar ages, although with different facies. Furthermore, raised marine deposits of MIS 11, MIS 9, MIS 7, and MIS 5 representing ancient beaches, or sandy bars that protected lagoons or marshes from direct sea influence outcropped in the area.

Even MISs can be correlated to erosive horizons (that separated the seismic units), reflecting lowstands. Thus, the shorelines associated with to MIS 14, MIS 12, MIS 10, MIS 8, and MIS 6 could be identified in the seismic profiles. In this regard, there appears to be a stratigraphical gap from the end of Pliocene to MIS 15 (Middle Pleistocene), as reflected by both onshore and offshore information.

Nevertheless, we cannot discard the presence of materials slightly older than MIS 15 inland, as it was not possible to obtain AAR ages from all the differentiated sedimentological units. However, these sediments accounted for 60 m of total thickness in the cores from La Mata and ca. 20 m in core AB-1.

It is noteworthy that onshore cores showed an absence of marine character deposits. In this regard, these cores varied from sabkha-marsh-coastal conditions to marsh-saline and marsh, thus implying that small morphological and environmental changes occurred along the coastline during odd MISs. However, there was one exception: in La Mata Basin, a marine bed near its western boundary presented abundant mollusk remains of unquestionable marine character belonging to MIS 5. These remains were linked to a marine ingression or an anomalous high-energy event (tsunami) related to the high seismicity of the zone (LM-2).

Geophysics demonstrated that Pleistocene offshore records, mostly in syncline areas, were arranged in progressive unconformities on Pliocene deposits. In addition, these minor deformation processes, linked to tardive Alpine tectonics, were responsible for the presence of ancient beach deposits raised tens of meters above its original elevation. Thus, in the different headlands, tectonic uplifting processes caused MIS 13 to MIS 5 deposits formerly found at the edge of the sea (beaches and bars) to rise. In this regard, undated raised deposits at higher elevations suggest the possible presence of older ones.

In the geophysical profiles that crossed the marine extensions of the anticlines responsible for the headland development, it was possible to observe the strong Pliocene-Pleistocene erosive unconformity and the marked faulting, which is still active, that created differentiated accommodation spaces for offshore sediment accumulation and, in some cases, deformation.

In conclusion:

- In the emerged area, there was a lack of Pleistocene age sediments from the end of the Pliocene until MIS 15. During this long period, only erosive processes took place, although the extent and magnitude remain unknown.
- In coincidence with the outset of a higher sea level during odd MISs, from MIS 15 to MIS 5, the lowlands became wetlands: lagoon, alluvial plain, carbonate marsh, and sabkha appeared on the coastline, although seawater never intruded into them. In fact, raised beach deposits of MIS 7 and MIS 5 marked the most internal position of the shoreline.
- We postulate that sandy bars older than MIS 7 and MIS 5, now observable only through marine seismic profiles, created and protected these wetlands.
- The persistence of the wetland environment records can be variable as they maybe eroded after the effects of neotectonics and/or sea level fall during even MISs episodes. However, sedimentary resilience was noticeable in some basins. Indeed, in Pego marsh, almost continuous sedimentation took place from MIS 15 to MIS 5 in a bar-protected scenario.
- Thus, in the Betic domain of the Iberian Mediterranean realm, subsident troughs and synclines were characterized by a dominance of wetland-like environments at least from MIS 15, while anticlines suffered uplift episodes, as attested by raised beach deposits.

CRediT authorship contribution statement

Trinidad Torres: Conceptualization, Funding acquisition, Writing – original draft, Supervision. **José E. Ortiz:** Investigation, Methodology, Writing – original draft, Funding acquisition. **Rosa Mediavilla:** Investigation, Methodology. **Juan I. Santisteban:** Investigation, Methodology. **Ana Blázquez:** Investigation, Methodology. **Francisco J. Sierro:** Investigation, Methodology. **Yolanda Sánchez-Palencia:** Investigation, Methodology. **Ignacio López Cilla:** Investigation, Methodology. **Rogelio de la Vega:** Investigation.

Declaration of competing interest

The authors declare that they have no known competing financial interests or personal relationships that could have appeared to influence the work reported in this paper.

Data availability

Data will be made available on request.

Acknowledgements

This paper was made possible by Grant PID2021-123549NB-I00 (Análisis ambiental del entorno costero del SE Ibérico y su dinámica poblacional antigua) funded by MCIN/AEI/10.13039/501100011033. We thank to the Department of the Ambient, Canvi Climatic i Desenvolupament Rural of the Generalitat Valenciana that gave the work permission in the protected area, to Francisco José Martínez García Director of the Parque Natural de las lagunas de La Mata y Torrevieja and to Ana María Colominas Cloquell Technician of "Espacios Naturales del Parque Natural de Las Lagunas de La Mata y Torrevieja" as well as to the members of the Interpretation Center at La Mata. We thank Prof. Perea for kindly providing us the seismic profile S-81B-07. We thank Prof. Fabrizio Marra and two anonymous reviewers for the revision of the paper.

Appendix A. Supplementary data

Supplementary data to this article can be found online at https://doi.org/10.1016/j.csr.2024.105198.

References

Alfaro García, P., Doménech, C., Estévez, A., Soria, J.M., 1995. Estructuras de deformación en sedimentos del Cuaternario reciente de la cuenca del Bajo Segura (Alicante). Discusión sobre su posible origen sísmico. Geogaceta 17, 91–94.

Alfaro, P., Andreu, J.M., Delgado, J., Estévez, A., Soria, J.M., Teixidó, T., 2002. Quaternary deformation of the Bajo Segura blind fault (eastern Betic Cordillera, Spain) revealed by high-resolution reflection profiling. Geol. Mag. 139, 331–341.

Alfaro, P., Andreu, J.M., Delgado, J., Martin-Rojas, I., Soria, J.M., Tent-Manclus, J.E., Fernández Mejuto, M., 2015. Historia geológica del valle de la Vega Baja del Segura. In: Ferrández Verdú, T., Diz Ardid, E. (Eds.), Historia Natural de la Huerta de Orihuela. Ayuntamiento de Orihuela, pp. 11–32.

Alfaro, P., Bartolomé, R., Borque, M., Estévez, A., García-Mayordomo, J., García-Tortosa, F., Gil, A., Gràcia, E., Lo Iacono, C., Perea, H., 2012. The Bajo Segura Fault zone: active blind thrusting in the eastern betic cordillera (SE Spain). J. Iber. Geol. 38, 271–284.

Alfaro, P., Estévez, A., Moretti, M., Soria, J.M., 1999. Structures sédimentaires de déformation interprétées comme séismites clans le quaternaire du bassin du bas Segura (Cordillère Bétique orientale). Comptes Rendus Acad. Sci. - Ser. IIA Earth Planet. Sci. 328 (1), 17–22.
Archivo Técnico de Hidrocarburos. http://hidrocarburos.mityc.es/ath/(accessed 27 June 2022).
Baena, J., García-Rodríguez, J., Maldonado, A., Uchupi, E., Udías, A., Wandossell Zamarreño, I., 1982. Mapa geológico de la plataforma continental española y zonas adyacentes. Almería-Garrucha and Chella-Los Genoveses. Servicio de Publicaciones Instituto Geológico y Minero de España, Madrid.
Bardají, T., Goy, J.L., Mörner, N.A., Zazo, C., Silva, P.G., Somoza, L., Dabrio, C.J., Baena, J., 1995. Towards a plio-pleistocene chronostratigraphy in eastern betic basins (SE Spain). Geodin. Acta 8 (2), 112–126.
Bellés, J., Mateu, F., Cuerda, J., 1978. Morfología cuaternaria de la costa entre l'Altet y el Cap de Santa Pola. Cuadernos de geografía 23, 63–82.
Bernat, M., Echailler, J.V., Busquet, J.C., 1982. Nouvelles datations Th-U sur des Strombes du Dernier Interglaciaire en Méditerranée. C.R. Acad. Sci. Paris II 295, 1023–1026.
Blázquez, A.M., 2005. Evolución cuaternaria de l'Albufera d'Elx: Paleoambientes y foraminíferos fósiles. Memorias del Museo Paleontológico de Elche.
Blázquez, A.M., Ferrer, C., 2003. L'Albufereta d'Alacant: foraminíferos y evolución paleoambiental. Cuaternario Geomorfol. 18 (3–4), 55–72.
Blázquez, A.M., Usera, J., 2010. Palaeoenvironments and quaternary foraminifera in the elx coastal lagoon (Alicante, Spain). Quat. Int. 221 (1–2), 68–90.
Blázquez, A.M., Usera, J., Ferrer, Y., 2000. Foraminíferos fósiles de un sondeo de la albufera cuaternaria de Elx-Santa Pola (Alicante, España): paleoecología e interpretación paleoambiental. In: Roselló, V.M. (Ed.), Geoarqueologia I Quaternari Litoral. Memorial MP Fumanal. Departament de Geografia, Universitat de València, Valencia, pp. 309–320.
Bright, J., Kaufman, D.S., 2011. Amino acid racemization in lacustrine ostracodes, part I: effect of oxidizing pre-treatments on amino acid composition. Quat. Geochronol. 6 (2), 154–173.
Caracuel, J.E., Corbí, H., Giannetti, A., Monaco, P., Soria, J.M., Tent-Manclús, J.E., Yébenes, A., 2011. Paleoenvironmental changes during the late Miocene (Messinian)–Pliocene transition (Bajo Segura Basin, southeastern Spain): sedimentological and ichnological evidence. Palaios 26 (12), 754–766.
Carbonel, P., 1985. Néogène. In: Oertli, H.J. (Ed.), Atlas des ostracodes de France. Bull. Centr. Rech. Explor, vol. 9. .-Prod. Elf-Aquitaine, pp. 311–335.
Catafrau, E., Gaytán de Ayala, M., Pereda, I., Vázquez, J.T., Wandossel, J., 1994. Mapa Geológico de la plataforma continental española y zonas adyacentes escala 1: 200.000 num 72 & 73. ITGE. 2 maps.
Causse, Ch, Goy, J.L., Zazo, C., Hillaire-Marcel, C., 1993. Potential chronologique (Th/U) des faunes Pléistocenes Mediterranéennes: example des terracesses marines des regions de Murcie et Alicante (South-Est de l'Espagne). Geodin. Acta 6, 121–134.
Collado, M.Á., Robles Cuenca, F., 1983. Estudio de las asociaciones de moluscos de la turbera holocena de Torreblanca (Castellón). Mediterránea Ser. Geol. 105–142.
Cuenca, A., Delgado, I., Doménech, C., Tomás, R., 2000. El Cuaternario reciente de la Vega Baja del Segura. Problemática geotécnica. In: Exma. Diputación provincial de Alicante. Itinerarios Geológicos de la Provincia de Alicante, Alicante, pp. 27–41.
Dabrio, C.J., Zazo, C., Cabero, J.L., Goy, J.L., Hillaire-Marcel, C., González-Delgado, J.A., Lario, J., Bardají, T., Silva, P.G., Borja, F., García-Blazquez, A.M., 2011. Millennial-scale sea level and climate fluctuations during the second highstand of MIS 5e. Quat. Sci. Rev. 30, 335–346.
D'Angelo, G., Gargiullo, S., 1987. Guida Alle Conchiglie Mediterranee: Conoscerle, Cercarle, Collezionarle. Fabbri.
De Santis, V., Caldara, M., Torres, T., Ortiz, J.E., Sánchez-Palencia, Y., 2018. A review of MIS 7 and MIS 5 terrace deposits along the gulf of Taranto based on new stratigraphic and cronological data. Ital. J. Geosci. 137, 349–368.
De Santis, V., Caldara, M., Torres, T., Ortiz, J.E., Sánchez-Palencia, Y., 2020. The role of beach ridges, spits, or barriers in understanding marine terraces processes on loose or semiconsolidated substrates: insights from the givoni of the Gulf of Taranto (southern Italy). Geol. J. 55, 2951–2975.
Dumas, B., 1981. La Région d'Alicante. In: Aguirre, E. (Ed.), Libro-Guía de la excursión-mesa redonda sobre el Tirreniense del litoral mediterráneo español. Internacional Quaternary Association, Lyon-Madrid, pp. 45–75.
Duque, C., Gómez-Fontalva, J.M., Murillo, J.M., Calvache, M.L., 2018. Assessing the uncertainties of the water budget in the Torrevieja aquifer (southeast Spain). In: Calvache, M.L., Duque, C. y, Pulido-Velázquez, D. (Eds.), Groundwater and Global Change in the Western Mediterranean Area. Springer, Cham, pp. 109–116.
Echailler, J.C., Lauriat, R., 1978. Decouverte d'un nouveau niveau marin d'age Calabrien sur le litoral mediterraneen d'Espagne (Province d' Alicante). C. R. Somm. Soc. Geol. Fr. 4, 178–180.
Ferrer, C., Blázquez, A.M., 1999. Algunos aspectos de la dinámica sedimentaria durante el Holoceno superior de un sector del Baix Vinalopó (Alicante). In: Pallí Buxó, L., Roqué Pau, C. (Eds.), Avances en el estudio del Cuaternario Español. AEQUA, Girona, pp. 99–105.
Ferrer, C., Blázquez, A.M., Esquembre, M.A., Ortega, J.R., 2005. Reconstrucción paleoambiental de l'Albufereta d'Alacant durante el período ibero-romano (500 a. C.-300 d.C. In: Sanjaume, E., Mateu, J.F. (Eds.), Geomorfologia Litoral I Quaternari, Homenatge Al Professor Vicenç M. Rosselló I Verger. Universidad de Valencia, Valencia, pp. 137–150.
Fontán, A., Muñoz, A., Muñoz-Martín, A., Rivera, J., Uchupi, E., 2013. The morpho-tectonic setting of the Southeast margin of Iberia and the adjacent oceanic Algero-Balearic Basin. Mar. Petrol. Geol. 45, 17–41.
Fumanal, M.P., Blázquez, A.M., Usera, J., Martínez, J., Ferrer, C., 1998. Resultados preliminares del estudio de los sondeos realizados en la albufera cuaternaria Elx-Santa Pola (Mediterráneo Occidental, España). In: Gómez-Ortiz, A., Franch, S. (Eds.), Investigaciones recientes de la geomorfología española, pp. 721–724.
Fumanal, M.P., Mateu, G., Rey, J., Somoza, L., Viñals, M.J., 1993. Las unidades morfosedimentarias cuaternarias del litoral del Cabo de la Nao (Valencia-Alicante) y su correlación con la plataforma continental. In: Fumanal, P., Bernabeu, J. (Eds.), Estudios sobre Cuaternario. Medios Sedimentarios, cambios Ambientales, Habitat Humano. Universidad de Valencia, Valencia, pp. 53–64.
Gaibar-Puertas, C., Barceló, J.C., 1969. Las playas de Cuaternario marino levantadas en el Cabo de Santa Pola (Alicante). Bol. Geol. Min. 53 (2), 105–121.
García-Mayordomo, J., Insua-Arévalo, J., Martínez-Díaz, J., Jiménez-Díaz, A., Martín-Banda, R., Martín-Alfageme, S., Álvarez-Gómez, J., Rodríguez-Peces, M., Pérez-López, R., Rodríguez-Pascua, M., Masana, E., Perea, H., Martín-González, F., Giner-Robles, J., Nemser, E., Cabral, J., Compilers, Q., 2012. The quaternary active faults Database of Iberia (QAFI v.2.0). J. Iber. Geol. 38, 285–302.
Giménez, J., Borque, M.J., Gil, A.J., Alfaro, P., Estévez, A., Suriñach, E., 2009. Comparison of long-term and short-term uplift rates along an active blind reverse fault zone (Bajo Segura, SE Spain). Studia Geophys. Geod. 53 (1), 81–98.
Gofas, S., Salas, C., Moreno, D., 2011. Moluscos marinos de Andalucía volumen 1. Universidad de Málaga servicio de Publicaciones e intercambio científico, Málaga.
Goodfriend, G.A., 1991. Patterns of racemization and epimerization of amino acids in land snail shells over the course of the Holocene. Geochem. Cosmochim. Acta 55, 293–302.
Goy, J.L., Hillaire-Marcel, C., Zazo, C., Ghaleb, B., Dabrio, C.J., González, A., Bardají, T., Civis, J., 2003. U-series ages of coral-bearing littoral deposits with Strombus bubonius of OIS 7 from La Marina (Alicante, SE Spain). A reappraisal of the Tyrrhenian chronostratigraphy in the Mediterranean Sea. Final Conf. Proj. IGCP 437, 109–111.
Goy, J.L., Zazo, C., 1987. Quaternary Shorelines and Their Deposition Related to the Continental Deposits and Neotectonics in the Elche Depression (Alicante, Spain). Abstr. 12th INQUA, Congress, Canada, p. 176.
Goy, J.L., Zazo, C., 1988. Sequences of quaternary marine levels in Elche Basin (eastern betic cordillera, Spain). Palaeogeogr. Palaeoclimatol. Palaeoecol. 68, 301–310.
Goy, J.L., Zazo, C., 1989. The role of neotectonics in the morphologic distribution of the Quaternary marine and continental deposits of the Elche Basin, southeast Spain. Tectonophysics 163 (3–4), 219–225.
Goy, J.L., Zazo, C., Hillaire-Marcel, C., 1986. Stratigraphie et chronologie (U/Th) du Thyrrénien du Sud-Est de l'Espagne. Z. Geomorphol. 62, 71–82.
Goy, J.L., Zazo, C., Somoza, L., Dabrio, C.J., 1990. Evolución paleogeográfica de la depresión de Elche-Cuenca del Bajo Segura (España) durante el pleistoceno. Estud. Geol. 46 (3–4), 237–244.
Gradstein, F., Ogg, J., Smith, A., 2004. A Geologic Time Scale 2004. Cambridge University Press, Cambridge.
Guillaume, M.C., Peypouquet, J.P., Tétart, J., 1985. Quaternaire et Actuel. In: Oertli, H.J. (Ed.), Atlas des Ostracodes de France. Bull. Cent. Rech. Explor. Prod. Elf-Aquitaine, vol. 9, pp. 337–377.
Hayward, B.W., Cedhagen, T., Kaminski, M., Gross, O., 2017. World Foraminifera Database. http://www.marinespecies.org/foraminifera. (Accessed 24 March 2017).
Hearty, P.J., 1986. An inventory of last interglacial (sensu lato) age deposits from the mediterranean basin. Z. Geomorphol. 62, 51–69.
Hearty, P.J., 1987. New data on the pleistocene of mallorca. Quat. Sci. Rev. 6, 245–257.
Hearty, P.J., Miller, G., Stearns, C., Szabo, B.J., 1986. Aminostratigraphy of quaternary shorelines in the mediterranean basin. Geol. Soc. Am. Bull. 97, 850–858.
Hemleben, C., Spindler, M., Anderson, O.R., 2012. Modern Planktonic Foraminifera. Springer Science & Business Media.
Hillaire-Marcel, C., Carro, O., Causse, Ch, Goy, J.L., Zazo, C., 1986. Th/U dating of *Strombus bubonus* bearing marine terraces in southeastern Spain. Geology 14, 613–616.
Howarth, R.J., McArthur, J.M., 1997. Statistics for strontium isotope stratigraphy: a robust LOWESS fit to the marine Sr-isotope curve for 0 to 206 Ma, with look-up table for derivation of numeric age. J. Geol. 105 (4), 441–456.
IGME-CSIC, 2022. Inventario de puntos de agua de la provincia de Alicante (España). datos.gob.es/es/catalogo/ea0010987-base-de-datos-de-puntos-de-agua-del-igme. (Accessed 18 October 2022).
Imbrie, J., Hays, J.D., Martinson, D.G., McIntyre, A., Mix, A.C., Morley, J.J., Pisias, N.G., Prell, W.L., Shackleton, N.J., 1984. The orbital theory of Pleistocene climate: support from a revised chronology of the marine δ O18 record. In: Berger, A., Imbrie, J., Hays, J., Kukla, G., Saltzman, B. (Eds.), Milankovitch and Climate. Series C: Mathematical and Physical Sciences, vol. 126. Kluwer Academic Publishers, Hingham, Mass, pp. 269–305.
Kaufman, A., Broecker, W.S., Ku, T.L., Thurber, D.L., 1971. The status of U-series methods of mollusc dating. Geochem. Cosmochim. Acta 60, 1115–1183.
Kaufman, D.S., 2000. Amino acid racemization in ostracodes. In: Goodfriend, G., Collins, M., Fogel, M., Macko, S., Wehmiller, J. (Eds.), Perspectives in Amino Acid and Protein Geochemistry. Oxford University Press, New York, pp. 145–160.
Kaufman, D.S., Manley, W.F., 1998. A new procedure for determining DL amino acid ratios in fossils using reverse phase liquid chromatography. Quat. Geochronol. 17, 987–1000.
Kennet, J.P., 1983. Neogene Planktonic Foraminifera. A Phylogenetic Atlas. Hutchinson Ross, New York.
Labeyrie, L.D., Duplessy, J.C., Blanc, P.L., 1987. Variations in mode of formation and temperature of oceanic deep waters over the past 125,000 years. Nature 327 (6122), 477–482.
Lambeck, K., Chappell, J., 2001. Sea level change through the last glacial cycle. Science 292 (5517), 679–686.
Lirer, F., Foresi, L.M., Iaccarino, S.M., Salvatorini, G., Turco, E., Cosentino, C., Sierro, F. J., Caruso, A., 2019. Mediterranean Neogene planktonic foraminifer biozonation and

biochronology. Earth Sci. Rev. 196, 102869 https://doi.org/10.1016/j.earscirev.2019.05.013.
Loeblich, A.R., Tappan, H., 1988. Foraminiferal Genera and Their Classification. Springer, New York, New York.
Martín-Martín, M., Guerrera, F., Tramontana, M., 2020. Tectono-sedimentary evolution of the cenozoic basins in the eastern external betic zone (SE Spain). Geosciences 10 (10), 394.
Martinez Solares, J.M., Mezcua Rodriguez, J., 2002. Catalogo sismico de la Peninsula Iberica (880 a.C.-1990). Monografía Núm. 18. Dirección General del Instituto Geográfico Nacional, Madrid.
McLaren, S.J., Rowe, P.J., 1996. The reliability of uranium-series mollusc dates from the western Mediterranean Basin. Quat. Sci. Rev. 15, 709–717.
Mediavilla López, R.M., Murillo Díaz, J.M., Santisteban Navarro, J.I., 2007. La estratigrafía en la modelación matemática de los acuíferos. El caso del embalse subterráneo de Torrevieja (Alicante). Bol. Geol. Min. 118, 709–724.
Montenat, C., 1973. Les formations néogenes et quaternaires du Levant espagnol. Ph D Dissertation. University of Paris.
Montenat, C., 1977. Les bassins néogènes du levant d'Alicante et de Murcia (Cordillères Bétiques orientales-Espagne). In: Stratigraphie, paléogéographie et évolution dynamique. Documents des Laboratoires de Géologie de la Faculté des Sciences de Lyon, Lyon.
Montenat, C., Ott d'Estevou, P.H., Coppier, G., 1990. Les bassins neógènes entre Alicante et Cartagena, vols. 12–13. Documents et travaux de l'Institut géologique Albert de Lapparent, pp. 313–368.
Murray-Wallace, C.V., Goede, A., 1995. Aminostratigraphy and electron spin resonance dating of Quaternary coastal neotectonism in Tasmania and the Bass Strait islands. Aust. J. Earth Sci. 42 (1), 51–67.
Ortiz, J.E., Torres, T., Julià, R., Delgado, A., Llamas, F.J., Soler, V., Delgado, J., 2004b. Numerical dating algorithms of amino acid racemization ratios from continental ostracodes. Application to the Guadix-Baza Basin (southern Spain). Quat. Sci. Rev. 23 (5–6), 717–730.
Ortiz, J.E., Torres, T., Julià, R., Llamas, F.J., 2004a. Algoritmos de cálculo de edad a partir de relaciones de racemización/epimerización de aminoácidos en pelecípodos marinos del litoral mediterráneo español. Rev. Soc. Geol. Espana 17 (3–4), 217–227.
Ortiz, J.E., Torres, T., Pérez-González, A., 2013. Amino acid racemization in four species of ostracodes: taxonomic, environmental, and microstructural controls. Quat. Geochronol. 16, 129–143.
Ortiz, J.E., Torres, T., Sánchez-Palencia, Y., Ferrer, M., 2017. Inter- and intra-crystalline protein diagenesis in *Glycymeris* shells: implications for amino acid geochronology. Quat. Geochronol. 41, 37–50.
Perea, H., Gràcia, E., Alfaro, P., Bartolomé, R., Iacono, C.L., Moreno, X., Masana, E., 2012. Quaternary active tectonic structures in the offshore Bajo Segura Basin (SE iberian peninsula–mediterranean sea). Nat. Hazards Earth Syst. Sci. 12 (10), 3151–3168.
Rabineau, M., Berné, S., Olivet, J.L., Aslanian, D., Guillocheau, F., Joseph, P., 2006. Paleo sea levels reconsidered from direct observation of paleoshoreline position during Glacial Maxima (for the last 500,000 yr). Earth Planet Sci. Lett. 252, 119–137.
Santisteban, J.I., Mediavilla, R., 2006. El acuífero de Torrevieja: estudio estratigráfico e implicaciones hidrogeológicas. Fondo documental del CN-IGME. Informe inédito.
Santisteban, J.I., Mediavilla, R., Martínez Santos, P., Castaño, S., Martínez Alfaro, P.E., Murillo, J.M., López Geta, J.A., Rodríguez, L., 2004. Nuevos datos sobre la estratigrafía de subsuelo del acuífero de Torrevieja (Alicante): implicaciones en el modelo conceptual de funcionamiento. Hidrogeología y Recursos Hidráulicos 27, 215–223.
Segura-Beltrán, F., Pardo-Pascual, J.E., 2019. Fan deltas and floodplains in Valencian coastal plains. In: Morales, J. (Ed.), The Spanish Coastal Systems. Springer, Cham, pp. 489–516.
Segura, F., Pardo, J.E., Sanjaume, E., 1997. Evolución cuaternaria de la albufera de Torreblanca. Cuaternario Geomorfol. 11 (1), 3–18.
Schiebel, R., Hemleben, C., 2017. Planktic Foraminifers in the Modern Oceans. Springer-Verlag GmbH Berlin Heidelberg.
Shackleton, N.J., 2000. The 100,000-year Ice-Age cycle found to lag temperature, carbon dioxide, and orbital eccentricity. Science 289, 1897–1902.
Silva, P.G., Bardají, T., Roquero, E., Martínez-Graña, A., Perucha, M.A., Huerta, P., Lario, J., Giner-Robles, J.L., Rodríguez-Pascua, M.A., Pérez-López, R., Cabero, A., Goy, J.L., Zazo, C., 2015. Paleogeografía sísmica de zonas costeras en la Península Ibérica: su impacto en el análisis de terremotos antiguos e históricos en España. Cuaternario Geomorfol. 29 (1–2), 31–56.
Silva, P.G., Goy, J.L., Somoza, L., Zazo, C., Bardají, T., 1993. Landscape response to strike-slip faulting linked to collisional settings: Quaternary tectonics and basin formation in the Eastern Betics, southeastern Spain. Tectonophysics 224 (4), 289–303.
Skene, K.I., Piper, D.J.W., Aksu, A.E., Syvitski, J, 1998. Evaluation of the global oxygen isotope curve as a proxy for Quaternary sea level by modeling of delta progradation. J. Sediment. Res. 68 (6), 1077–1092.
Somoza, L., 1993. Study of the Quaternary coast between Cabo de Palos and Guardamar (Murcia-Alicante) regarding the variations of sea level in relation to the geodynamic context. Spec. Issue. Boletín Instituto Oceanográfico 12, 4.
Somoza, L., Bardají, T., Dabrio, C.J., Goy, J.L., Zazo, C., 1986. Análisis de secuencias de islas barrera pleistocenas en relación con variaciones del nivel del mar, laguna de La Malta (Alicante). Acta Geol. Hisp. 21 (1), 151–157.
Soria, J.M., Alfaro, P., Estévez, A., Delgado, J., Duran, J.J., 1999. The Holocene sedimentation rates in the lower Segura Basin (eastern Betic Cordillera, Spain); eustatic implications. Bull. Soc. Geol. Fr. 170 (3), 349–354.
Soria, J.M., Alfaro, P., Ruiz Bustos, A., Serrano, F., 1996. Organización estratigráfica y bioestratigrafía del plioceno en el borde sur de la Cuenca del Bajo Segura (sector de Rojales, Alicante), cordillera Bética Oriental. Estud. Geol. 52 (3–4), 137–145.
Storms, J.E., Weltje, G.J., Terra, G.J., Cattaneo, A., Trincardi, F., 2008. Coastal dynamics under conditions of rapid sea-level rise: late Pleistocene to Early Holocene evolution of barrier–lagoon systems on the northern Adriatic shelf (Italy). Quat. Sci. Rev. 27 (11–12), 1107–1123.
Tabares, P., Martínez-Santos, P., Martínez-Alfaro, P.E., 2009. Modelización 3D del acuífero Terciario de Torrevieja. Geometría del acuífero. Bol. Geol. Min. 120 (1), 53–60.
Tent-Manclús, J.E., 2012. Modelización del cambio de la línea de costa en la comarca del Bajo Segura (Sinus Ilicitanus, S Provincia de Alicante) en los últimos 15.000 años. Cidaris 31, 51–62.
Tent-Manclús, J.E., 2013. Cambio de la línea de costa en el Bajo Segura (Sur de Alicante) en los últimos 15.000 años. Estud. Geográficos LXXIV (275), 683–702.
Tent-Manclús, J.E., Soria, J.M., 2014. Formación y desecación del sinus ilicitanus (Sur de Alicante) en los últimos 15.000 años. Geogaceta 55, 35–38.
Tent-Manclús, J.E., Soria, J.M., Viseras Alarcón, C., 2014. Modelo geológico 3D del NO de la Cuenca del Bajo Segura (Alicante, SE de España). Geogaceta 55, 11–14.
Torres Pérez-Hidalgo, T.J., Puche Riart, O., Ortiz Menéndez, J.E., Arribas, I., Vega Panizo, R.D.L., 2006. Biometría de Strombus bubonius Lamark 1791 del yacimiento de Cerro Largo (Roquetas de Mar, Almería). Geogaceta 40, 167–170.
Torres, T., Llamas, J., Canoira, L., Coello, F.J., García Alonso, P., Ortiz, J.E., 2000. Aminostratigraphy of two pleistocene marine sequences from the mediterranean coast of Spain: Cabo de Huertas (Alicante) and Garrucha (Almería). In: Goodfriend, G.A., Collins, M.J., Fogel, M.L., Macko, S.A., Wehmiller, J.F. (Eds.), Perspectives in Amino Acids and Protein Geochemistry. Oxford University Press, New York, pp. 263–278.
Torres, T.D., Llamas, J.F., Canoira, L., García-Alonso, P., García-Cortés, A., Mansilla, H., 1997. Amino acid chronology of the lower pleistocene deposits of venta micena (Orce, Granada, Andalusia, Spain). Org. Geochem. 26 (1–2), 85–97.
Torres, T., Ortiz, J.E., Arribas, I., 2013. Variations in racemization/epimerization ratios and amino acid content of Glycymeris shells in raised marine deposits in the Mediterranean. Quat. Geochronol. 16, 35–49.
Torres, T., Ortiz, J.E., Arribas, I., Delgado, A., Julia, R., Martín-Rubí, J.A., 2010. Geochemistry of persististrombus latus gmelin from the pleistocene Iberian Mediterranean realm. Lethaia 43 (2), 149–163.
Torres, T., Ortiz, J.E., Blázquez, A.M., Ruiz Zapata, B., Gil, M.J., Martín, T., Sánchez-Palencia, Y., 2015. The MIS 5 palaeoenvironmental record in the SE mediterranean coast of the Iberian Peninsula (río Antas, Almeria, Spain). Clim. Past Discuss 11 (4), 3897–3936.
Torres, T., Ortiz, J.E., Martín-Sánchez, D., Arribas, I., Moreno, L., Ballesteros, B., Estrella, T.R., 2014. The long Pleistocene record from the Pego-Oliva marshland (Alicante-Valencia, Spain). Geol. Soc. Spec. Publ. 388 (1), 429–452.
Torres, T., Ortiz, J.E., Mediavilla, R., Sánchez-Palencia, Y., Santisteban, J.I., Vega-Panizo, R., 2022. Assessment of prospective geological hazards in Torrevieja-La Mata coast (western Mediterranean) based on Pleistocene and Holocene events. Nat. Hazards 111 (3), 2721–2748.
Torres, T., Ortiz, J.E., Sánchez-Palencia, Y., Ros, M., Navarro, F., López-Cilla, I., Blázquez, A., 2020. The pleistocene and Holocene records of the Mazarrón basin (SE Spain). Quat. Int. 566, 256–270.
Usera, J., Blázquez, A.M., Guillem, J., Alberola, C., 2002. Biochronological and paleoenvironmental interest of foraminifera lived in restricted environments: application to the study of the western Mediterranean Holocene. Quat. Int. 93–94, 139–147.
Usera, J., Blázquez, A.M., Guillem, J., Alberola, C., 2006. Evolución holocena de la Marjal de Peñíscola (Castellón, España) deducida del estudio de sus foraminíferos fósiles. Rev. Espanola Micropaleontol. 38 (2–3), 381–393.
Viñals, M.J., 1995a. Secuencias estratigráficas y evolución morfológica del extremo meridional del Golfo de Valencia (Cullera-Dénia). In: Quaternari, Grup Valencià (Ed.), El Cuaternario del País Valenciano. University of Valencia, Valencia, pp. 163–167.
Viñals, M.J., 1995b. Formaciones litorales fósiles en la costa de Moraira (Alicante). En El Cuaternario del País Valenciano. In: Quaternari, Grup Valencià (Ed.), El Cuaternario del País Valenciano. University of Valencia, Valencia, pp. 187–192.
Waelbroeck, C., Labeyrie, L., Michel, E., Duplessy, J.C., Mcmanus, J.F., Lambeck, K., Labracherie, M., 2002. Sea-level and deep water temperature changes derived from benthic foraminifera isotopic records. Quat. Sci. Rev. 21 (1–3), 295–305.
Zazo, C., 1999. Interglacial sea levels. Quat. Int. 55, 101–113.
Zazo, C., Goy, J.L., Dabrio, C.J., Bardají, T., Hillaire-Marcel, C., Ghaleb, B., González-Delgado, J.A., Soler, V., 2003. Pleistocene raised marine terraces of the Spanish Mediterranean and Atlantic coasts: records of coastal uplift, sea-level highstands and climate changes. Mar. Geol. 194, 103–133.
Zazo, C., Goy, J.L., Hoyos Gómez, M., Dumas, B., Porta, J., Martinell, J., Aguirre, E., 1981. Ensayo de síntesis sobre el Tirreniense peninsular español. Estud. Geol. 37, 257–262.
Zazo, C., Goy, J.L., Somoza, L., Dabrio, C.J., 1990. Evolution of barrier Island-lagoon systems from 200 KA Ago to the present in the littoral zone of Alicante (Spain). Impact of a probable sea level rise. In: Paepe, R., Fairbridge, R.W., Jelsgersma, S. (Eds.), Greenhouse Effect, Sea Level and Drought. NATO ASI Series (Series C: Mathematical and Physical Sciences), vol. 325. Springer, Dordrecht, pp. 439–446.